Spring 2014

Techno-economic and life-cycle modeling and analysis of various energy storage technologies coupled with a solar photovoltaic array

Brian Andrew Peterson

Department:

TECHNO-ECONOMIC AND LIFE-CYCLE MODELING AND ANALYSIS OF VARIOUS ENERGY STORAGE TECHNOLOGIES COUPLED WITH A SOLAR PHOTOVOLTAIC ARRAY

by

BRIAN ANDREW PETERSON

A THESIS

Presented to the Graduate Faculty of the

MISSOURI UNIVERSITY OF SCIENCE AND TECHNOLOGY

In Partial Fulfillment of the Requirements for the Degree

MASTER OF SCIENCE IN CHEMICAL ENGINEERING

2014

Approved by

Dr. Joseph. D. Smith, Advisor
Dr. Douglas Ludlow
Dr. Suzanna Long

ABSTRACT

Renewable energies, such as wind and solar, are a growing piece of global energy consumption. The chief motivation to develop renewable energy is two-fold: reducing carbon dioxide emissions and reducing dependence on diminishing fossil fuel supplies. Energy storage is critical to the growth of renewable energy because it allows for renewably-generated electricity to be consumed at times when renewable sources are unavailable, and it also enhances power quality (maintaining voltage and frequency) on an electric grid which becomes increasingly unstable as more renewable energy is added. There are numerous means of storing energy with different advantages, but none has emerged as the clear solution of choice for renewable energy storage.

This thesis attempts to explore the current and developing state of energy storage and how it can be efficiently implemented with crystalline silicon solar photovotlaics, which has a minimum expected lifetime of 25 years assumed in this thesis. A method of uniformly comparing vastly different energy storage technologies using empirical data was proposed. Energy storage technologies were compared based on both economic valuation over the system life and cradle-to-gate pollution rates for systems with electrochemical batteries.

For stationary, non-space-constrained settings, lead-acid batteries proved to be the most economical. Carbon-enhanced lead-acid batteries were competitive, showing promise as an energy storage technology. Lithium-ion batteries showed the lowest pollution rate of electrochemical batteries examined, but both lithium-ion and lead-acid batteries produce comparable carbon dioxide to coal-derived electricity.

ACKNOWLEDGEMENTS

This thesis would not have been possible without the knowledge and support of my advisor Dr. Joseph D. Smith. He welcomed me into his research group at Missouri S&T's Energy Research and Development Center (ERDC) with open arms and constant encouragement. He recognized my passion for energy as the defining issue of our time and provided me with a project that allowed me to contribute to that area of research. Certainly without him, none of this would have been possible.

I would like to show my thanks to Dr. Douglas Ludlow for being a member of my advisory committee and contributing to the completion of this thesis. Additionally, I would like to thank Dr. Ludlow for being a very helpful advisor during my undergraduate studies at Missouri S&T. He has been a valuable part of my education for many years.

Also, I would like to thank Dr. Suzanna Long, another member of my advisory committee. As a member of the Engineering Management Department, she offered a unique, cross-discipline perspective that was invaluable to finalizing my research.

This project was supported either technically or financially or both by some businesses. Steve O'Rourke and Marc Lopata of Microgrid Solar, Michael Nispel of C&D Technologies, and The Doe Run company all played crucial roles in this thesis.

I am forever grateful to my parents Steve and Debbie, my siblings John, Katie, and Jim for forming who I am today. I would like to thank all of my friends and family for their constant encouragement and support. Also, I must thank all the members of the ERDC who have been constantly helpful in all areas, research and otherwise.

TABLE OF CONTENTS

Page

LIST OF ILLUSTRATIONS

Figure Page

LIST OF TABLES

NOMENCLATURE

Symbol	Description
abs(x)	Absolute value of ‘x’
AC	Alternating current
CAES	Compressed air energy storage
CapEx	Capital expense
CdTe	Cadmium Telluride thin film solar photovoltaic cell
CIGS	Copper indium gallium diselenide
CIS	Copper indium diselenide
CVD	Chemical vapor deposition
DC	Direct current
DOD	Depth of discharge
ECDL	Electrochemical double layer
ERDC	Energy Research and Development Center
ESS	Energy storage size
GHG	Greenhouse Gas
HOMER	Hybrid Optimization Model for Electric Renewables
HTSE	High temperature steam co-electrolysis
Li-Ion	Lithium-ion battery
NPV	Net present value
NREL	National Renewable Energy Laboratory
O&M	Operating and maintenance
OFAT	One-factor-at-a-time
OpEx	Operating and maintenance expense
Pb-A	Lead-acid battery

Pb-C	Carbon-enhanced lead-acid battery
PCS	Power control system
PECVD	Plasma-enhanced chemical vapor deposition
PHES	Pumped hydroelectric energy storage
PSOC	Partial state of charge
PV	Photovoltaic
S-S	Sulfur-sodium battery
SOC	State of charge
UPS	Uninterruptable power supply
V-Redox	Vanadium redox battery
Zn-Br	Zinc bromide battery

1. INTRODUCTION

1.1 BACKGROUND

Access to robust and reliable energy is critical to modern society and ways of life around the world. Cheap, readily available energy is one of the most significant factors contributing to overall quality of life. Presently its world feeds the desire for energy almost entirely from fossil resources such as coal, crude oil, and natural gas. These energy resources have been heavily exploited over the past 150 years and have led the world through an industrial revolution and into a modern era of rapidly evolving technologies.

For all of the benefits that fossil fuels have brought, they are not without negative externalities[1]. Fossil fuels are not equally distributed over the globe. A large portion of proven crude oil reserves are controlled by countries in the Middle East. It is no coincidence that this region has had serious conflicts and wars fought over these resources. Society values fossil resources and the quality of life they bring. Control and influence over these valuable resources is of paramount importance to countries around the world, such as the United States. Energy independence is sought by virtually every government, and those counties that cannot achieve this goal from their own resources seek energy security for their people from other countries, which often leads to conflict. This cycle has and will continue as countries continue to seek energy security.

[1] Externality: "a side effect or consequence of an industrial or commercial activity that affects other parties without this being reflected in the cost of the goods or services involved…" [51].

Additionally, the combustion of fossil fuels leads to the emission of pollutants. A chief concern in today's world is the heavy emissions of carbon dioxide, produced when fossil fuels, primarily made of carbon, are burned. Carbon dioxide is a greenhouse gas (GHG) so increasing atmospheric concentrations are expected to lead to increased trapping of solar radiation-borne heat, thus raising global atmosphere temperatures. Rapid increases (by geological time) in global temperature could lead to a variety of environmental and climate changes such as rising sea level, flooding, drought, extreme weather, and species extinctions. The extent to which human activity through burning fossil fuels is contributing to global warming and climate change is a hotly debated topic. Regardless of scientific opinion, the effects are very hard to measure, especially given such a short snapshot (150 years), geologically speaking. However, it is clear that burning fossil fuels is increasing the carbon dioxide content of Earth's atmosphere. Preparations and research for worst-case scenarios should be undertaken.

Globally there has been a steady focus on developing and implementing renewable energy generation (wind and solar) technology. The motivation has been to reduce dependence on limited fossil fuel resources and to mitigate carbon dioxide emissions. Wind and solar are both robust energy sources which are accessible virtually anywhere, and at least one, if not both, can be plentiful nearly all regions. Renewable energy is also valuable in that they support small distributed generation facilities can easily be installed. This is especially true for solar, allowing residential, commercial, and industrial users to install supplemental generation in grid-connected scenarios. Additionally, renewable energy can be used to generate electricity remotely where the infrastructure costs of extending the grid are prohibitive. Renewable energy certainly has

a key role in the global energy portfolio that is slowly reducing the fraction of fossil-based energy usage.

The main drawback of wind and solar is their intermittent, non-dispatchable nature, whereas fossil-based electricity generation can be ramped up and down with demand. Renewables do not offer that same flexibility. Also fossil fuels can be transported from areas rich in resources to areas where electricity generation is needed, but non-dispatchable renewable energy must be generated using local resources. Intermittency leads to two primary problems: grid voltage/frequency instability and time of use discrepancy. Wind energy is much more variable and unpredictable than solar. Wind generation comprises a much larger portion of grid-level electricity than solar (3.46% vs. 0.11% of U.S. electricity generation in 2012) [1]. Total renewable power generation capacity is expected to increase 1.6% annually through 2040 [2]. This large and growing portion of renewable energy creates many issues including greater frequency and voltage instability. For grid-isolated renewable energy systems, time of use is of critical importance, as wind and/or solar may not be able to always meet demand. Both grid instability and time of use issues can be solved by energy storage.

There are numerous energy storage technologies: electrochemical batteries, flow batteries, flywheels, capacitors, pumped hydroelectric energy storage (PHES), compressed air energy storage (CAES), and others. Each technology has its own advantages and disadvantages. In general, periodic dips in grid voltage and frequency, increasingly caused by unpredictable renewable energy, can be alleviated by drawing electricity from energy storage, especially those technologies that have rapid response times. Many storage technologies have response times of less than 1 second which is

much better than a coal-fired power plant which takes about 10 seconds to respond to frequency dips [3] [4].

In addition to maintaining power quality, energy storage is used to supply electricity at a time of use when generation may be insufficient. PHES accounts for a large portion of global energy storage and is discharged to meet peak demand during the day while being charged overnight at base load generation levels [5]. This same time of use principle can be applied for more sporadic renewable electricity generation. Although PHES is only applicable on large scales (grid power supply) and not ideal for distributed or deployable solar photovoltaic (PV) generation, many other storage technologies have been explored and implemented to create continuous power supply from solar PV generation. Determination of the ideal energy storage technologies for implementations dedicated to crystalline silicon solar PV electricity generation together with an evaluation and recommendation for future analysis of energy generation-storage hybrid systems are the main subject of this thesis.

1.2 RESEARCH OBJECTIVES

The work and research done for this thesis was intended to meet the following objectives:

1. Survey the existing literature to investigate the following:
    a. The current state of solar PV technology.
    b. Current and developing energy storage technologies.
    c. Techniques for estimating energy storage lifetime.
    d. Comparative analyses of available energy storage technologies.

2. Identify and collect accurate and applicable sources of hourly solar PV output data and hourly demand data from a specific region.
3. Determine the best software tools for modeling a proposed solar PV-energy storage hybrid system.
4. Develop an hour-by-hour simulation of the hybrid system that incorporates an established method for uniformly estimating the lifetimes of various energy storage technologies with vastly different mechanisms of function.
5. Compare energy storage technologies over an assumed 25 year system lifetime using economic feasibility and environmental sustainability metrics.
6. Document and publish the work in a peer-reviewed literature journal article.

This thesis has effectively accomplished these research objectives. The details of the methodology, the results, and the conclusions and recommendations will be presented in the following sections.

2. LITERATURE REVIEW

2.1 BACKGROUND

Nations around the world are expanding renewable energy, including solar energy, since it can lead to increased energy independence and energy security as well as diminish the amount of GHG emissions. Currently many technologies exist to capture sunlight and convert it to usable forms of energy.

It is clear that energy storage will play a vital role in the growth and success of renewable solar energy because of its intermittent, non-dispatchable nature. Various in-use and developing energy storage technologies have various advantages, disadvantages, and viable applications. Understanding the current state of solar energy with energy storage is critical to moving the current state of electricity generation into the future.

2.2 SOLAR ENERGY

The sun is the supreme energy source for planet Earth. Solar energy is accessible nearly anywhere and can be harnessed to some degree on a daily basis. It is the energetic basis for nearly all natural biological activity on our planet and is becoming an important part of the world's energy portfolio. There are many ways in which solar energy can be harnessed.

2.2.1 Solar Thermal. The sun's radiant heat energy (infrared) is often directly absorbed and converted to thermal energy. This energy can then be used to heat media from near ambient up to 1,000 °C. Solar collectors and concentrators of various designs

can yield vastly different thermal efficiencies. Simple solar space and water heaters have been widely used for many years but only utilize lower temperature ranges (100-200°F). At the higher temperature ranges, solar thermal energy has been used to desalinate and disinfect water, to aid in thermochemical processing, to produce steam for electrical generation, or stored as sensible, latent, or chemical heat. Solar thermal is a viable use of solar energy, but it is not the focus for this work [6].

2.2.2 Solar Photovoltaics (PV). These are a class of technologies that directly convert solar energy into electricity. When photons contact a surface, electrons become excited, with a portion of the incident radiation converted to heat, re-emitted as light, or absorbed resulting in a chemical change. Certain materials when connected to a closed circuit allow the excited electrons to move through the circuit, creating an electric current. This photovoltaic effect was first described by Edmond Becquerel in 1839 [7]. The first viable silicon solar cell was developed in 1954 [7]. The efficiency and cost of solar cells have been the primary focus of research and innovation. Today there are numerous materials used to produce solar cells with varying efficiencies, costs, and growth prospects [7].

2.2.2.1 Materials. Silicon crystal-based solar PV cells are the most common material used in solar PV applications. As of 2010, they accounted for 83% of the solar PV market [8]. These systems consist of a junction of p-type and n-type silicon. In a basic cell, the silicon is metallized to conduct the electric current, and an anti-reflective coating increases absorbance which maximizes photons striking the silicon cell. The silicon can be made from slices of a silicon crystal, or ingot, which is grown from a single silicon seed crystal placed in molten silicon and slowly drawn out. This type of

solar cell is commonly referred to as a monocrystalline solar cell, which has the highest conversion efficiency of crystalline silicon solar cells (14-20%), however they are more costly. A cheaper alternative is polycrystalline silicon which is made by melting and re-casting the waste from monocrystalline cell production (usually from the electronics industry). Polycrystalline silicon solar cells have lower efficiencies (13-15%) and higher efficiency variability. The third method of producing silicon for solar PV cells is to ribbon cast the silicon. Rather than casting a cylindrical ingot and slicing into wafers, silicon is cast in a continuous sheet. This is a newer method and saves on production waste [8] [9].

Alternatively, silicon may be used in its amorphous (not crystalline) form for solar PV. A “thin film” of amorphous silicon is applied to a substrate, such as glass, plastic, or metal via plasma-enhanced chemical vapor deposition (PECVD). The layer may only need to be one micron thick, hence thin film. Because of material conservation this technology is proving to be cost effective, but the efficiencies of these solar cells (6-9%) are significantly less than those of crystalline silicon [9] [10].

Another material used to produce thin film solar cells is cadmium telluride (CdTe). CdTe is deposited onto a substrate by one of several methods: close space sublimation, vapor transport deposition, sputtering, electro depositions, or high vacuum evaporation. Also chalcopyrite-type compounds are used to produce thin film solar cells. Copper indium diselenide (CIS) and copper indium gallium diselenide (CIGS) are also used as thin film materials which are applied by chemical vapor deposition (CVD). CdTe and CIS/CIGS thin film solar cells have slightly higher efficiencies (9-11%, 10-12% respectively) than amorphous silicon thin film [9] [11] [12].

There are also other less common solar PV cell technologies being developed including. Organic solar PV cells use carbon-based molecules such as polymeric fullerene. The organic material can be applied to a substrate by printing, vacuum evaporation, or roll-to-roll coating. Because of how they are produced, organic solar cells are flexible and easy to incorporate into construction material or even clothing. These cells have seen practical efficiencies as high as 8% [13]. Also there are mesoscopic or dye-sensitized cells. These consist of essentially a layer of titanium dioxide and a layer of dye. They have relatively low efficiencies (7%), but can be made of many different colors and can even be transparent. Dye-sensitized cells have aesthetic appeal in architecture as windows. These cells also have military applications as camouflage [9] [14]. Sliver cells are another emerging technology developed at the Australian National University. They are made of extremely thin monocrystalline silicon. They are bifacial (convert light from both directions) and have efficiencies as high as 13.8%. Sliver cells are flexible and transparent, giving them the potential for architectural applications as well [9]. Research is also being done to improve solar concentrator technology. This technology usually consists of lenses and/or mirrors that increase the amount of photons striking the solar cell which increases electricity production. Unfortunately, there are issues with the durability of the solar concentrators and cooling of the solar cells [9] [15]. Recent work has been done using quantum design and nanostructure technology to maximize solar cell efficiency [15]. A family tree of the various materials used in solar PV is shown in Figure 2.1.

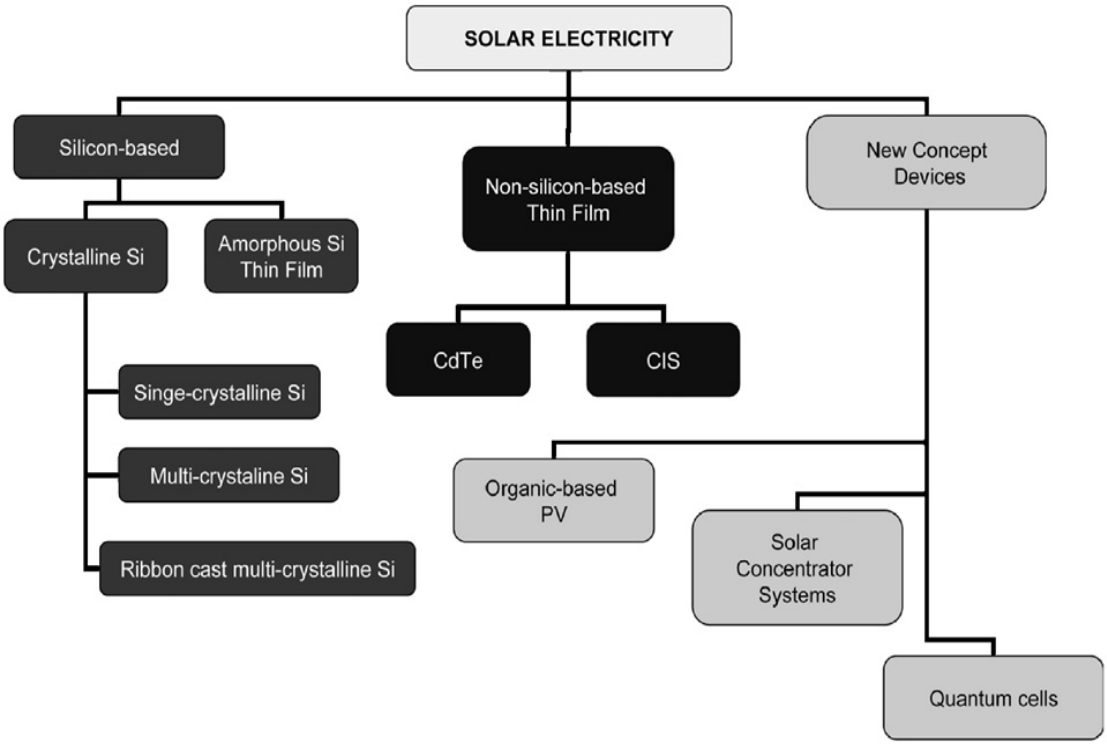

Figure 2.1: Family tree of solar photovoltaic materials **[15]**.

2.2.2.2 Design. An additional consideration in solar PV design is how the module is to be mounted. Commonly, solar PV arrays are fixed to a roof or a rack, usually on a tilt facing the Earth's equator to maximize electricity output. Alternatively, the solar PV array is mounted on mechanical devices that move the module using sun-tracking. Sometimes the mechanical mount is on only one axis, following the sun east to west. Other, more sophisticated devices also track the sun's azimuth. Sun-tracking can significantly improve the solar cell output, but they require significant additional energy, material, installation, and maintenance costs [9].

Another critical component of a solar PV array is the inverter setup. Inverters convert the direct current (DC) electricity produced by the solar cells to alternating current (AC), which is needed for most applications. The most basic inverter design involves a string inverter where all solar PV modules are connected on one "string" running to the single inverter. String inverters are susceptible to failure if any one module fails causing the entire string to fail. Alternatively there are multi-string inverters which connect inputs from multiple strings to separate inverters. These are slightly more reliable than single string inverters because one module failing only causes its particular string to fail, as opposed to the whole array. For larger arrays, central inverters can be used. These have multiple strings running to one inverter. The newest development in inverters is modular or micro-inverters. Each solar PV module has its own micro-inverter. They are generally more expensive, but have higher efficiency (87% for microinverters vs. 77% for string inverters) and are not susceptible to one module crashing the whole system [9] [16].

Inverters are one among many factors that determine a solar PV systems derate. The derate is the ratio of usable AC electricity to the DC electricity produced by the solar cell. Other factors contributing to solar PV efficiency include the transformer, mismatch of PV module current-voltage characteristics, diodes and connections, wiring, soiling (foiling) from dirt and debris on the solar panel itself, system availability, and shading [17].

2.2.2.3 Simulating solar photovoltaics. Simulating the production of solar PV electricity from empirical solar radiation data is fairly straight forward. There are two components of solar radiation: direct beam and diffuse. Direct beam radiation is

dependent on the sun shining clearly on the cell and the angle on which it strikes the cell. Diffuse radiation is not dependent on the incident angle and can even pass through thin clouds. Solar radiation is usually measured in terms of energy per time per area. A pyranometer can measure the global radiation, that is the sum of direct beam and diffuse radiation. A shaded pyranometer can measure the diffuse radiation by blocking the direct beam of the sun. A pyrheliometer is capable of measuring only direct beam radiation [18].

Additionally, cell temperature affects the cell efficiency. Air temperature, wind speed, precipitation, and direct vs. diffuse insolation all affect the cell temperature [9].

The National Renewable Energy Laboratory (NREL) has a freely available online application called PVWatts which can output annual, monthly, and hourly solar PV production for a specific location given certain defined system parameters. PVWatts was used to obtain data used in the scenarios examined in this paper [17].

2.3 ENERGY STORAGE TECHNOLOGIES

2.3.1 Electrochemical Batteries. There are two varieties of electrochemical batteries. Primary batteries, which cannot be recharged, are not of any concern for this paper as they have no energy storage applications for residential or grid applications. Secondary batteries however can be recharged and are a very common means of energy storage [5]. A basic scheme of an electrochemical battery can be found in Figure 2.2.

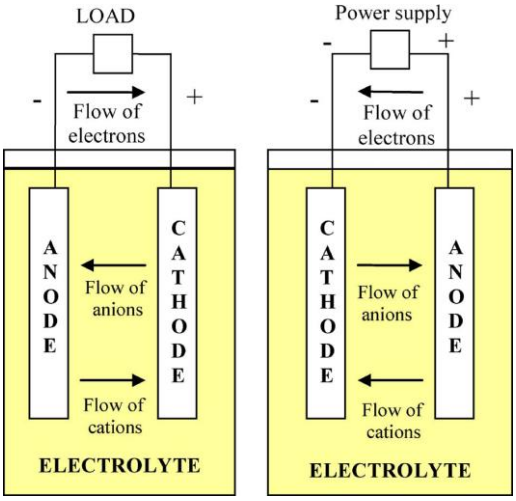

Figure 2.2: Discharging and charging (left and right, respectively) of an electrochemical battery **[20]**.

2.3.1.1 Lead-acid batteries. This is the oldest and most widely used chemistry of electrochemical batteries. The cathode is made of lead dioxide; the anode is made of lead; and sulfuric acid is the electrolyte. There are two main types of lead acid batteries: flooded and valve-regulated. Flooded require periodic watering to replace water that has "gassed" off from electrolysis. Valve-regulated lead-acid batteries capture and recombine the evolved oxygen and hydrogen. They are more expensive up front but require less maintenance. Lead-acid batteries have low capital and operating costs and high round trip efficiency (electricity out/electricity in), but they have short lifetimes [19] [20].

2.3.1.2 Lithium-ion batteries. These have a lithiated metal oxide for the cathode and graphite carbon for the anode. Presently there are numerous electrolytes being used and/or researched for current lithium-ion technology. Rather than a typical electrochemical reaction, lithium ions de-intercalate from the graphite and intercalate into

the lithiated metal oxide when discharging. The opposite is true for charging. They have low energy density and specific energy, making them ideal for portable and/or small applications, like laptop or cell phone batteries. The main drawback of lithium-ion batteries is the high capital cost which stems from the scarcity of lithium [19] [20] [5].

Lithium-ion batteries have not yet seen wide-spread use in large-scale applications. This is due to the fact that the technology is still not fully mature, especially from a safety perspective. Lithium-ion batteries have been known to catch on fire because of issues with material stability at high temperatures and short circuits within the cells that can cause a thermal runaway. These are areas of continuing research and improvement [21].

2.3.1.3 Sulfur-sodium batteries. These offer a slightly different design. The cathode and anode are liquid metals, made of sodium and sulfur respectively. The liquids are separated by the electrolyte-acting solid alumina ceramic. The basic setup of a sulfur-sodium battery can be seen in Figure 2.3. The main drawback of sulfur-sodium batteries is that they have to be maintained at about 300°C. The high temperature causes the batteries to have a large self-discharge rate. They are only economically viable on large-scale stationary applications. They are best used with existing grid infrastructure to help meet peak demand and control power quality [19] [20] [22]. For energy storage purposes, Duke Energy plans to install a 36 megawatt sulfur-sodium battery as part of a 153 megawatt wind farm in Texas [23].

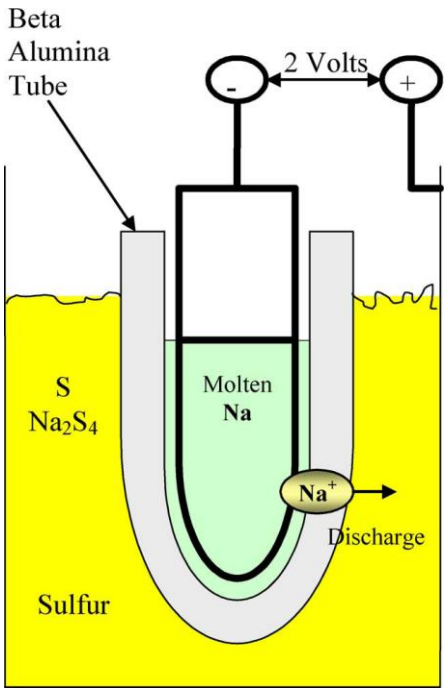

Figure 2.3: Basic operation of a sulfur-sodium cell **[20]**.

2.3.1.4 Carbon-enhanced lead-acid batteries. These have similar characteristics to traditional lead-acid batteries with the exception of cycle life. The addition of carbon at the lead anode improves cycle life tenfold in some cases. Carbon prevents deposits on the electrodes, a major mode of lead-acid battery failure, from forming on the anode. It also appears that lead-carbon batteries have increased lifetime at a partial state of charge (PSOC) compared to traditional lead-acid batteries. Lead-carbon batteries have many potential applications: hybrid/electric vehicles, UPS, grid-scale energy storage and frequency regulations, and remote power supply [19] [20] [24] [25].

2.3.1.5 Other electrochemical batteries. It is important to note that there are a variety of other electrochemical battery chemistries which will not be analyzed in this

paper. Nickel-cadmium batteries have a similar level of maturity as lead-acid batteries. They were commonly found in portable hand tools and were being applied in electric vehicles during the 1990's. Nickel-cadmium technology has since fallen out of style for two reasons: there have been growing concerns over the recyclability and toxicity of cadmium, and the more portable lithium-ion batteries became a fairly mature and widespread technology in the 2000's. Interestingly, the Golden Valley Electric Association in Fairbanks, Alaska claims to have built the world's highest power battery array from nickel-cadmium batteries. The system is rated at 40 MW for 7 minutes and has a 20 year system lifetime [5]. Additionally there are nickel-metal hydride and nickel-zinc batteries with similar properties to nickel-cadmium batteries.

Sodium-nickel chloride batteries are similar in nature to sulfur-sodium batteries but are a less mature technology. The primary difference between the two is that the anode is liquid nickel chloride rather than liquid sulfur. Sodium-nickel chloride batteries also have a higher cell voltage. They have better safety characteristics than sulfur-sodium batteries and have been shown to have applications in the automotive industry, but they have not been heavily researched for grid-level energy storage [5].

Also there are silver based batteries such as silver-zinc, silver-cadmium, and silver-hydrogen, which have silver oxide as the anode, with various cathodes. There are metal-air batteries: zinc-air, cadmium-air, and aluminum-air. Zinc-chloride and zinc-bromide batteries comprise the zinc-halogen class of batteries. Finally there are alkaline manganese batteries [26].

2.3.2 Flow Batteries. Another means of chemically storing energy is in what are called flow batteries. When discharging, flow batteries pump two electrolyte reagents into a fuel cell which contains ion selective membranes, generating electricity. When charging, the current applied reverses the reactions, moving ions back across the membrane as stored electrochemical potential. Flow batteries are advantageous in that the energy storage sizing (reactant tanks) can easily be done independent of power sizing (fuel cell size). Also, they have significantly longer cycle life than their electrochemical counterparts. A downside of flow batteries is that they are fairly complicated and have significant parasitic energy losses related to operating pumps, valves, etc. Flow battery technology has not been fully developed. Currently, these devices are available commercially on a small scale and are being tested on larger-scale demonstrations. Commercial applications could include peak demand support and load leveling on the utility scale, and as load leveling and seasonal energy storage for small grids and stand-alone renewable energy systems. There are multiple chemistries used in flow batteries, most of which have been developed over the past 25 years including vanadium redox, zinc bromide, polysulphide bromide, and zinc cerium among others [5]. The first two are a focus of flow battery analysis considered in this thesis. Growth and innovation in flow batteries has been limited by few developers and difficulty gaining market share over other energy storage technologies [5] [19] [27] [28]. The design of a flow battery can be seen in Figure 2.4.

2.3.2.1 Vanadium redox batteries. One flow battery chemistry that has seen significant real world applications involves vanadium redox batteries. These devices are slightly more costly than zinc bromide batteries, but are slightly more efficient as well.

Vanadium redox flow batteries are unique in that they use only one element. Vanadium works because it has 4 oxidation states. The anolyte side contains V^{2+}/V^{3+}, and the catholyte side contains V^{4+}/V^{5+}. During charging, an applied voltage allows electrons to move across the membrane such that V^{2+} and V^{5+} increase in concentration and V^{3+} and V^{4+} decrease. The opposite is true when discharging, creating a voltage, and current can flow [5] [19] [27] [28] [29].

2.3.2.2 Zinc bromide batteries. Another slightly cheaper but less efficient flow battery uses the zinc bromide chemistry. These contain $ZnBr_2$ on both sides of a membrane which allows Br^- to pass through. The anode side contains solid Zn, and the cathode side contains molecular bromine, Br_2. Concentrations of zinc and bromine increase and $ZnBr_2$ decreases when charging, and the opposite is true for discharging [5] [19] [27] [28] [30].

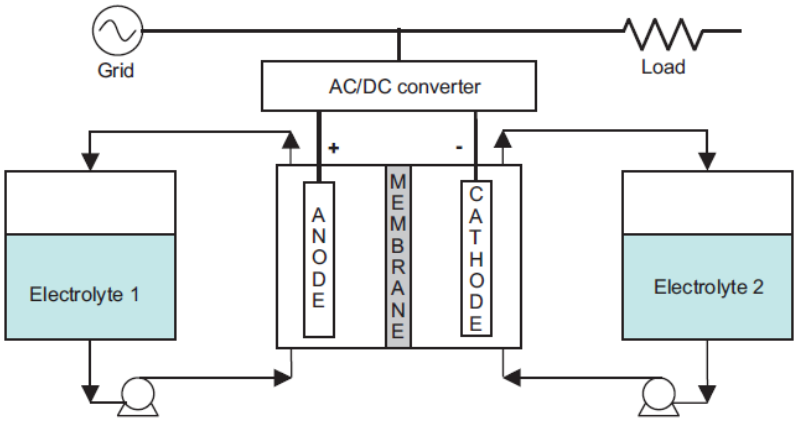

Figure 2.4: Flow battery setup **[5]**.

2.3.3 Mechanical Energy Storage. Aside from electrochemical batteries, another energy storage technology involves mechanical energy storage. Flywheels store energy as angular momentum. A large heavy wheel rotates rapidly. The stored energy of that system is a function of the angular velocity and moment of inertia of the wheel. It spins faster via an electric motor when charging and slows down as it discharges energy through an electric generator. A key advantage of flywheels is rapid discharging (high power output) and charging. Flywheels also have virtually limitless cycle life and typically reach their calendar lifetime (usually 20 years) first [19] [20] [5].

2.3.3.1 Low-speed flywheels. Typically made of steel, low-speed flywheels can commonly be found in industrial high power applications. Low-speed flywheels slowly accumulate energy, spinning up to 6000 RPM, and discharging it quickly for high power demands. Low-speed flywheels are not usually considered for energy storage and were not considered as part of this thesis [5] [19] [20].

2.3.3.2 High-speed flywheels. More advanced flywheels spin up to 50,000 RPM in a vacuum or helium chamber. High-speed flywheels are made of composite, light-weight, and/or high strength materials as well as ultra-low friction assemblies and bearings. They have large parasitic energy losses due to pumping requirements to maintain a vacuum. This thesis focuses on high-speed flywheels because they are more useful for energy storage. From this point forward any reference to flywheels assumes the high-speed variety. Because of their characteristics, flywheels are best served in high cycle rate applications such as grid-scale frequency regulation rather than medium- to long-term energy storage. Flywheels have relatively high capital and operating costs [5] [19] [20]. The basic design of a high-speed flywheel can be seen in Figure 2.5.

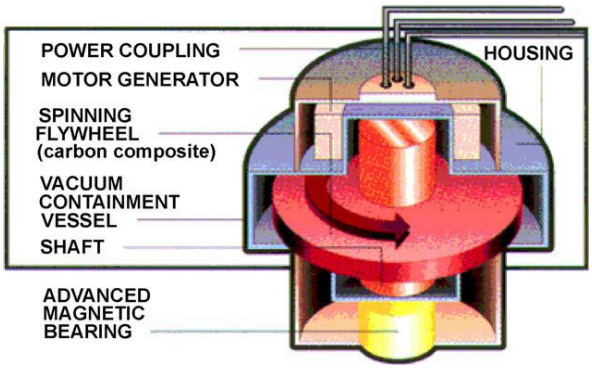

Figure 2.5: High-speed flywheel setup **[20]**.

2.3.4 Electrostatic Energy Storage (Supercapacitors). Capacitors function by separating a oppositely charged surfaces with an insulating dielectric layer. This electrostatic energy storage can cycle almost limitlessly with negligible degradation. They are able to charge and discharge very rapidly. Traditional capacitors are typically found in small-scale applications.

Supercapacitors are a developing method of storing electric energy. They consist of high very high surface area electrode material, such as activated carbon with a molecule-thin electrolyte layer as the dielectric separator. Maximizing the surface area increases the energy density of supercapacitors compared to traditional capacitors. Electrochemical double layer supercapacitors (ECDL) are the most common supercapacitors because they have the lowest manufacturing costs and will be studied in this paper. Figure 2.6 shows an ECDL cell. There are also hybrid capacitors and pseudo-capacitors. Supercapacitors show promise in more high-power, short-duration applications, providing short-term peak shaving as well as power (not energy) supply in UPS systems. Some research is being done in hybridized energy storage/UPS with

batteries and supercapacitors where the high-cycle life supercapacitors meet short term power/energy needs and batteries meet long duration energy needs. Supercapacitor technology is limited due to the high capital cost and low energy density and will not likely penetrate the energy storage market until costs are dramatically reduced [20]. Figure 2.7 shows a family tree of various supercapacitors.

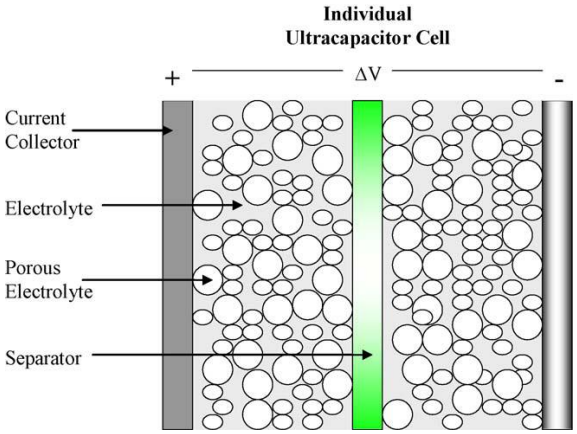

Figure 2.6: ECDL supercapacitor cell **[20]**.

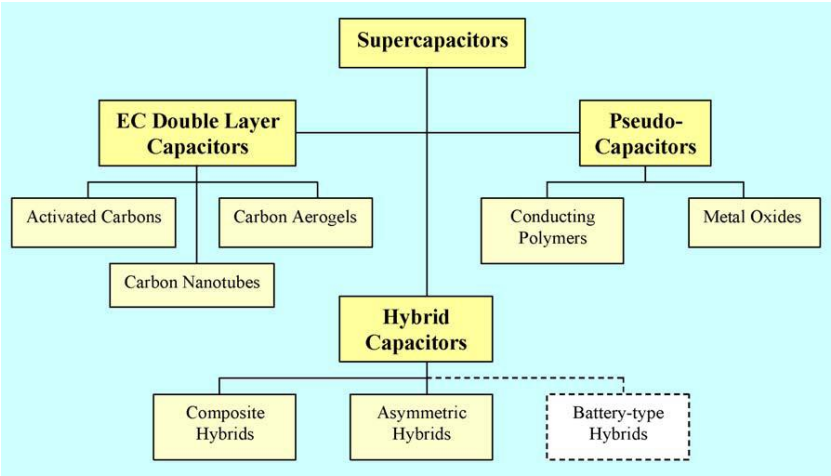

Figure 2.7: Supercapacitor family tree **[20]**.

2.3.5 Potential Energy Storage. Potential energy is usually stored on a large scale by either PHES or CAES. The downside to both PHES and CAES is that they are typically limited to large-scale applications and are geographically limited. For this study of more deployable forms of energy storage, PHES and CAES will be omitted, but they will be discussed below.

2.3.5.1 Pumped hydroelectric energy storage (PHES). In PHES, excess energy is used to pump water to an elevated reservoir which can be natural or man-made. When electricity is needed, water is used to drive turbines much like hydroelectric dams. PHES is one of the most widely implemented energy storage technologies with some 90 GW of installed capacity globally as of 2008. Of local interest to the author, Ameren Missouri uses the Taum Sauk PHES plant for helping meet peak demand during the day and recharging/refilling overnight [5] [19] [20] [31]. PHES design can be seen in Figure 2.8.

2.3.5.2 Compressed air energy storage (CAES). CAES utilizes air-tight underground compartments such as abandoned mines, aquifers, or hollowed out salt domes. Excess energy is used to drive compressors which pump pressurized air up to 75 bar into the underground chamber. To extract the energy, the compressed air is combined with a small amount of fuel, usually natural gas, and is ignited and expanded through a series of turbines [5] [19] [20] [31]. CAES design can be seen in Figure 2.9.

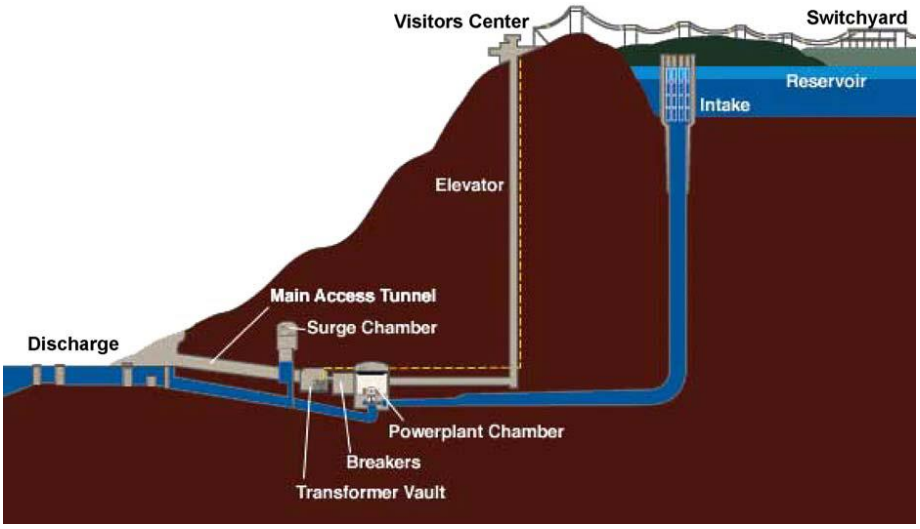

Figure 2.8: Pumped hydroelectric energy storage setup **[20]**.

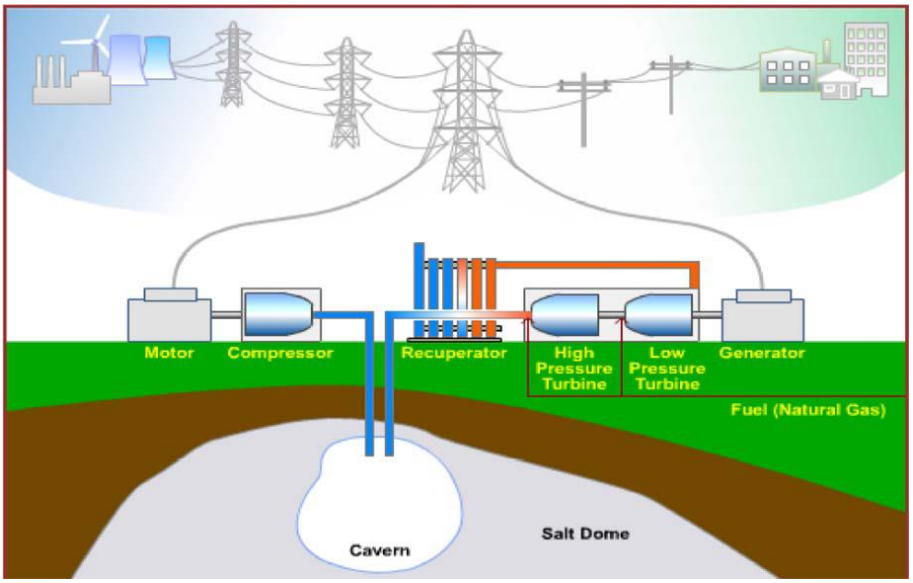

Figure 2.9: Compressed air energy storage setup **[20]**.

2.3.6 Hydrogen Storage. Several methods have been developed to produce hydrogen, a readily usable reactant for energy storage. Steam and methane can be reacted with a catalyst to produce hydrogen and carbon dioxide (methane reforming). This is called steam methane reforming and is very common in industry. Coal, hydrocarbons, or biomass can be "gasified" by combusting in a less-oxygen-rich or oxygen-absent environment, producing carbon monoxide and hydrogen. Another method involves electrolysis, where electricity is used to separate hydrogen and oxygen from water. There is also the newer, more efficient high temperature steam co-electrolysis (HTSE). There are a number of other hydrogen production methods that involve biological processes, solar electrochemical processes, and others. There are opportunities to store renewable energy as hydrogen, but the low density of hydrogen presents issues with the physical storage [32].

Pressurization and adsorption in metal hydrides are the most developed methods of hydrogen storage. For pressurization, steel tanks can be used up to 250 bar, but are typically very heavy. Lighter/stronger carbon composite materials have been developed to pressurize hydrogen up to 350 bar. To be competitive with other energy storage technologies, 700 bar storage pressure is needed. Metal hydrides composed of nickel and aluminum readily adsorb hydrogen and restore it to the gaseous state under temperature changes, offering potential as hydrogen storage. Other hydrogen storage technologies being developed include liquefaction and adsorption in carbon nanotubes. Because hydrogen storage technologies are far from maturity, they are not analyzed in this thesis [20].

2.4 MODELING ENERGY STORAGE PERFORMANCE

There are two general classes of methods for calculating and estimating battery and/or energy storage lifetime. There are performance degradation models and post-processing models. The former uses real-time performance indicators (usually voltage) in combination with measured capacity and estimated life remaining. Since these models require the inputs of real data as the energy storage system ages, they are not easily applied in long time scale predictive modeling which is the topic of this thesis. However, post-processing models are applicable for modeling because they simply use nameplate values of the energy storage to estimate life remaining and need no feedback of data on degrading performance [33]. Post-processing models are discussed below.

2.4.1 Cycle Counting. This method assumes that each discharge-charge cycle represents a certain fraction of the storage system's lifetime. There are several factors to be accounted for in this form of modeling including depth of cycles, speed of cycles, and overcharging. Cycle lifetime of batteries is usually determined by experimental repetitive cycling at a set depth of discharge (DOD) until failure. This experiment is repeated at various depths of discharge, and a curve can be fit to the data. Experimentally this is very reproducible and predictable, but real world applications, especially coupling with renewable energy, can pose difficulties. Energy storage for renewable energy may remain at a PSOC for extended periods making the counting of cycles arbitrary at best. This method is more suited for uninterruptible power supply settings where discharge-recharge cycles are very clear [33].

2.4.2 Throughput Counting. This method assumes that an energy storage system only has a set amount of energy that can be run through it until failure. Of course

maintaining PSOC, deep cycling, and over charging are factors that may be accounted for in some way. Throughput lifetime is usually an extension of cycle life in that the throughput life is found by multiplying the number of cycles by the depth of the cycles and by the nameplate capacity of the energy storage. This can be averaged over various depths of discharge or factors can be estimated as a function of DOD. Throughput lifetime is much more practical to use in determining energy storage lifetime for application in renewable energy, especially in long-time scale predictive models. A version of this method is used in NREL's Hybrid Optimization Model for Electric Renewables (HOMER) software. Throughput counting will be used in this thesis [33].

3. TECHNO-ECONOMIC ANALYSIS

3.1 INTRODUCTION

Current and developing deployable energy storage technologies include: electrochemical batteries, flow batteries, flywheels, and supercapacitors. Determining the most economical option for a stand-alone solar PV and energy storage microgrid of off-grid homes hinges primarily on the size (and therefore cost) of the energy storage and how often it will be replaced. Estimating the needed size and frequency of replacement for the energy storage is difficult given the variable nature of solar energy. Further complicating this process is the fact that electrochemical batteries behave much differently than flywheels which behave much differently than supercapacitors.

This work utilized a uniform comparison methodology to determine which energy storage technology provided the best economic performance using a 10-home stand-alone solar PV and energy storage microgrid as a basis. Additionally, a sensitivity analysis on the basic factors affecting the cost of such a system was performed.

3.2 METHODOLOGY

3.2.1 System Perfomance. This thesis studied a theoretical grid-isolated solar PV-energy storage system to provide electricity to 10 average Missouri homes in St. Louis, MO. Many considerations were taken in how to model the hourly state of the system. Numerous input variables were required

3.2.1.1 Solar photovoltaic data. To develop a comparison of energy storage technologyies, the hourly solar PV output data was needed. NREL's PVWatts online application was identified as an excellent source of hourly solar PV data for a crystalline silicon array with user-defined variables as inputs: location, DC power rating, DC to AC derate, array tilt and azimuth. The location selected was St. Louis, MO; DC power rating was set to 100 kW (the outputs could then be prorated to different sizes); DC to AC derate was 0.87 (higher than PVWatts' standard 0.77, but reasonable given advances in microinverter technology); array tilt of 15° was selected as most reasonable for both roof and ground mount systems, and an azimuth of 180° (South) was used to maximize production [16] [17].

It was also important to account for degradation of the solar panel over time. Silicon panels' output has been observed to decline by about 0.5% annually [34]. This degradation was applied to all hourly output values in the n^{th} hour, according to Equation 3.1:

$$\text{Solar Generation(n)} = \text{Solar Generation(n)} * (1 - \text{n} * \frac{0.005}{8760}) \quad (3.1)$$

A system lifetime of 25 years was used for the present study. One year data were repeated to create a full 25 year profile of electricity generation. Leap years were ignored so that each year was 8760 hours.

3.2.1.2 Demand data. The next step was to determine the hourly demand profile. Any profile of demand would likely need repeating to fit the number of hours in the solar PV electricity generation profile. For this study, the one-year average hourly use of a Missouri resident was selected [35]. Also electricity consumption growth was accounted

by using projected annual change in electricity demand. Residential electricity usage was projected to decrease by 0.2% annually through the year 2040 [2]. This was applied to demand in the n^{th} hour, shown in Equation 3.2:

$$\text{Demand(n)} = \text{Demand} * (1 - \text{n} * \frac{0.002}{8760}) \tag{3.2}$$

With both generation and demand profiles established, the energy deficit or surplus at each hour was calculated. An energy surplus was sent to energy storage, unless energy storage was full, then the excess energy was lost. Energy was drawn from storage during a deficit.

Additionally, the maximum power demand for the load had to be determined. The data was only given in hourly increments. The data is read as an average power (kW) for one hour (producing a kilowatt-hour value of energy demand). Of course there are spikes in power usage over any given hour. To determine the maximum power demand, the maximum hourly value was multiplied by a so-called "power demand factor" which is the assumed ratio of maximum power demand to average power demand over a given hour span. For this analysis, a factor of 1.5 was used for a residential power load. Commercial, industrial, and grid loads would require a power demand factor of 2 or even much higher.

This power demand factor characterized the maximum rate of discharge, but did not account for charge rate. Since solar energy is very steady, this maximal charge rate defined from hourly data was a valid representation of the maximum instantaneous charge rate and needed no similar "factor" applied to it. A critical assumption required

that the energy storage could charge at all rates defined by energy surpluses (kilowatt-hours per hour).

3.2.1.3 Energy storage sizing. For this simulation, energy storage size (kWh) was calculated by using the energy surpluses and deficits as well as the characteristic round-trip efficiency and self-discharge rate of the particular energy storage technology being considered. The calculation had to be iterated because energy storage self-discharge is a function of the unknown energy storage size.

A maximum DOD was defined as 80% for all storage technologies except sulfur-sodium batteries and flywheels. This value was chosen because most battery systems are considered "dead" when they reach 80% of their rated capacity, and battery manufactures usually determine the cycle life at 80% DOD [33] [36]. However, 90% maximum DOD was used for sulfur-sodium batteries and flywheels. This was because the model could not converge on a solution with 80% maximum DOD because sulfur-sodium battery's and flywheels' large self-discharge rates were so high that they could not meet the energy demand with the largest permissible solar PV array.

To begin the calculation, the maximum state of charge[2] (SOC) was set as zero and the initial energy storage size was set to be zero. First, the energy surplus/deficit was added/subtracted to/from the SOC and self-discharge was assumed to be zero in this initial energy storage sizing. Energy added to storage was "taxed" at the round-trip efficiency value of the given storage technology by multiplying the energy surplus by that efficiency. SOC was not to exceed its initial value of zero, so all SOCs were less than

[2] State of charge (SOC): the remaining charge of an energy storage system expressed in either absolute energy (kWh) or a percentage.

or equal to zero. The absolute value of the SOC divided by the maximum DOD was evaluated at every hour of the system lifetime (219,000 hours/25 years), defining the energy storage size. If this value increased at any subsequent hour, the larger value was stored as the new energy storage size. This value was used to determine self-discharge in any hour.

Recall that the first iteration of the energy storage sizing calculation was done with a self-discharge rate of zero. The same energy storage sizing procedure was performed, but this time real self-discharge values were incorporated. Of course the energy storage size can increase through the simulation and probably will when including self-discharge. If the energy storage size at the end of the sizing procedure did not match the energy storage size from the beginning, the procedure had to be run again using the newest energy storage size value. The energy storage sizing procedure was repeated until the energy storage size value converged. Once the model converged, the minimum necessary energy storage size to meet energy demand without violating the minimum DOD was determined.

The following list is a list of the main steps involved in the energy storage sizing procedure described in the previous four paragraphs:

1. Values for round-trip efficiency, self-discharge rate, maximum DOD as well as the 219,000 hourly energy surplus/deficits were obtained.
2. 219,000 non-positive SOC values were determined by starting at zero then adding or subtracting the energy surpluses and deficits from the previous SOC from hour 1 to hour 219,000, but when adding surpluses, SOC was not allowed to be greater than zero. A new value for energy storage size was

stored when an abs(SOC)/maxDOD value exceeded a previous energy storage size.

3. Step 2 was repeated except self-discharge was subtracted from the SOC at each hour as well.
4. Step 3 was repeated until the ending value and beginning value for energy storage size were within one kWh of each other, signifying convergence of the energy storage size

The iterative flow chart scheme representation of the above list of steps can be seen in Figure 3.1.

3.2.1.4 Energy storage lifetime. One method for determining energy storage lifetime, especially electrochemical batteries, is cycle lifetime (how many cycles of discharging a certain percent of its capacity and recharging to full capacity can be completed before the storage is deemed no longer useful). Cycle lifetime can vary significantly with different depths of discharge during the cycles. Any energy storage for a stand-alone solar PV-storage system will almost certainly have highly variable DOD and often will stay at a PSOC rather than fully recharging. This makes estimating storage lifetime by counting cycles very difficult. Rather than a cycle lifetime approach, energy throughput lifetime was used.

The energy throughput method uses a specific amount of ampere-hours of electricity or kilowatt-hours of energy that can be discharged from the storage before it is deemed no longer useful [33]. This was determined for various storage technologies by multiplying the storage capacity by the cycle lifetime by the maximum DOD. Also, most storage technologies have an expected calendar life regardless of how little it is used.

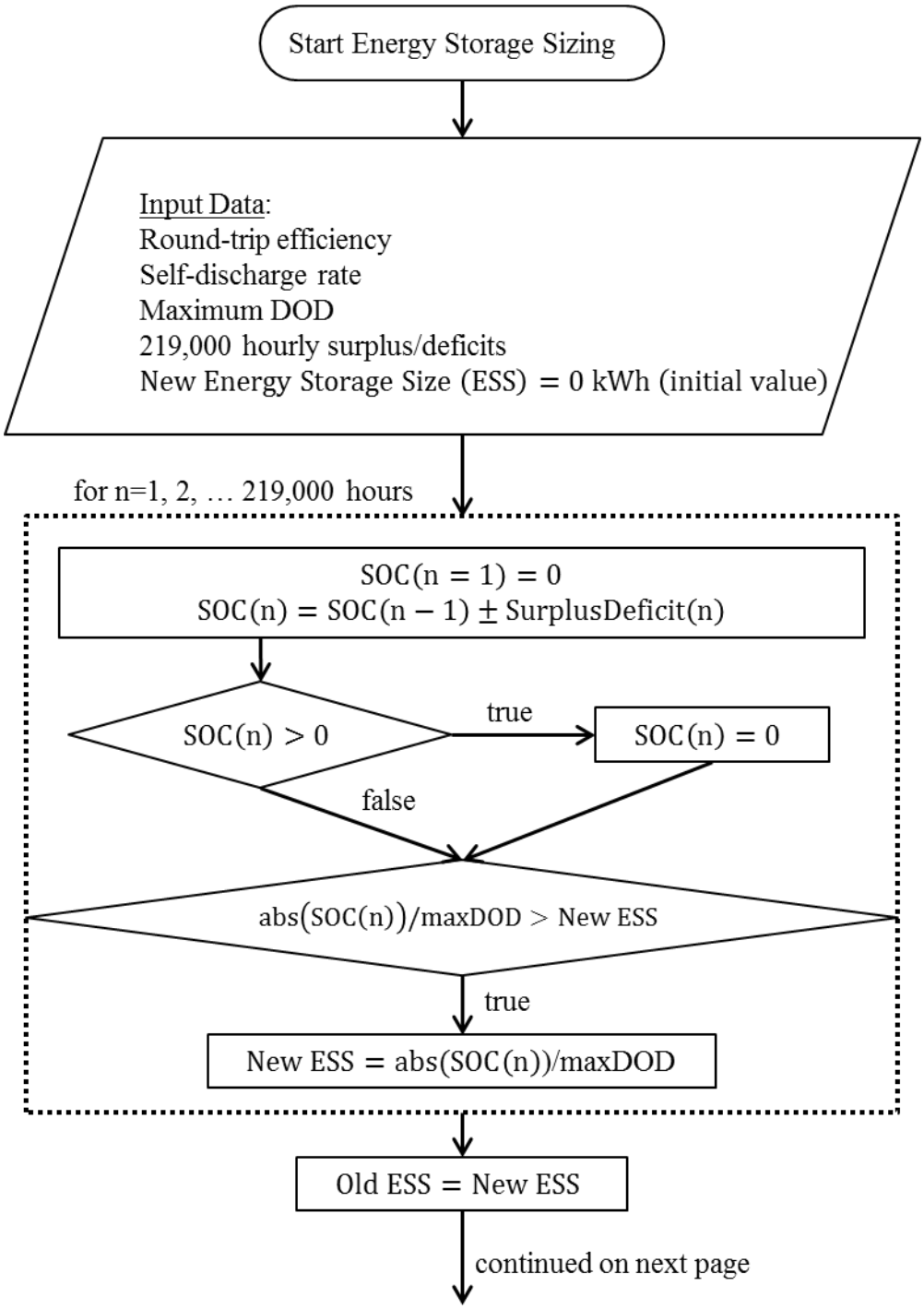

Figure 3.1: Flow chart of the energy storage sizing procedure. Note that when an energy surplus is added to the SOC, it is decreased by multiplying by the round-trip efficiency. This flow chart continues onto the next page.

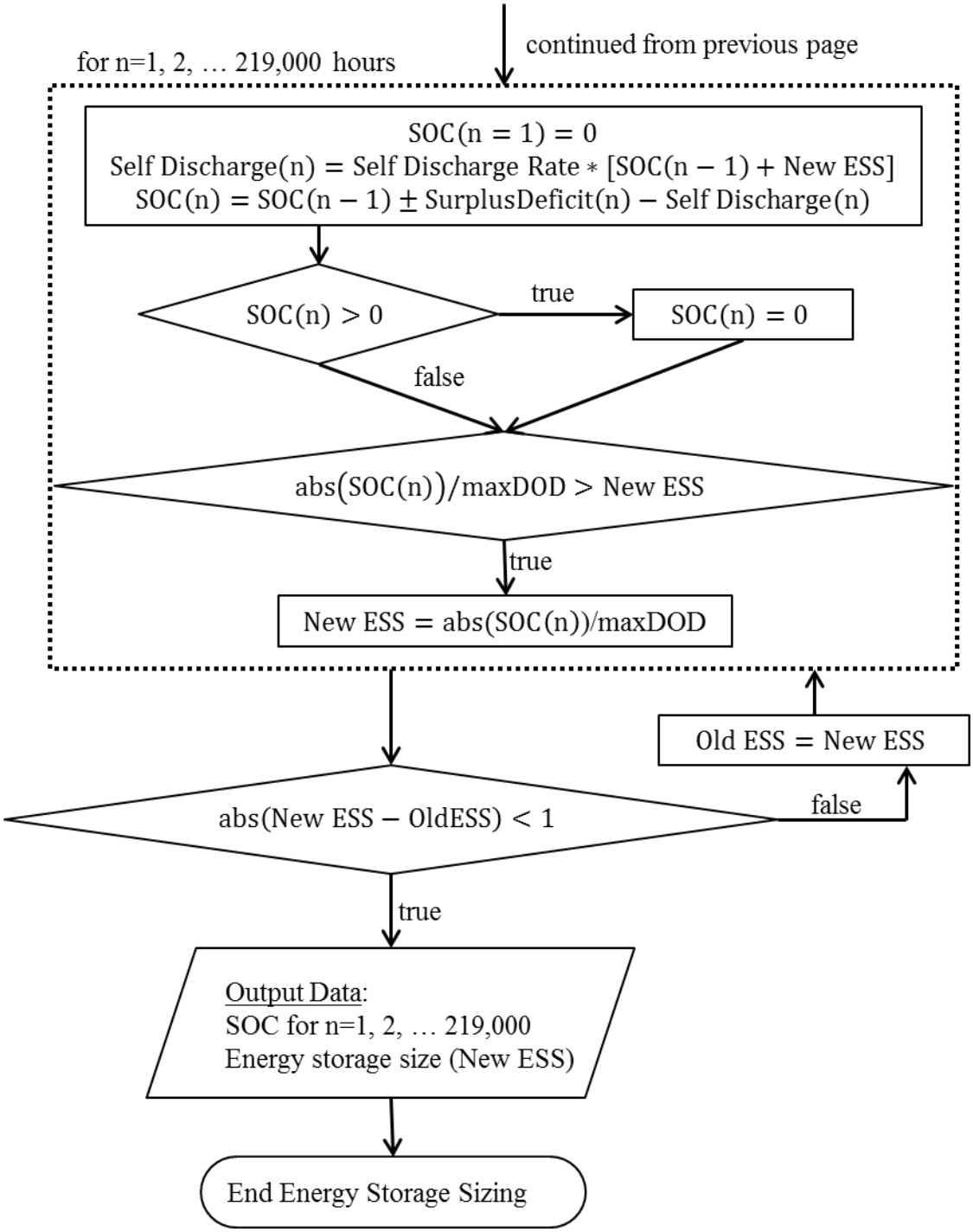

Figure 3.1: Flow chart of the energy storage sizing procedure (continued). Note that when an energy surplus is added to the SOC, it is decreased by multiplying by the round-trip efficiency.

Replacement occurred once either the throughput life or calendar life has expired, unless the time remaining in the system lifetime (25 years) was 10% or less of the calendar lifetime value.

Some of the values in Table 3.1 vary widely. This is because within each class of energy storage technology there are numerous different designs and factors that can influence their performance. For the sake of the study, the lowest values for round-trip efficiency and cycle life were used. The lowest value for self-discharge was used. For calendar life, one quarter of the range was added to the minimum and rounded down to the nearest integer. The exact values of performance characteristic used are in Table 3.2.

3.2.2 Economic Analysis. To study the economic performance of each system, cash flows for each month were to be calculated. The first step was to estimate capital and operating expenses of the components of the system. The solar PV array cost can be estimated on a basis of present value dollar per installed kilowatt capacity. The installed cost used for this analysis was $3,330 per kW capacity [16] [37]. This could then be used to calculate the capital cost of the PV array. Operating and maintenance (O&M) expenses (OpEx) were assumed to be negligible for the solar array.

Capital expenses (CapEx) for energy storage was calculated in two parts: the amount of energy (kWh) that can be stored and the power (kW) or rate at which that energy can be discharged [38]. This cost occurs in the initial cash flow period and at each subsequent replacement months. Additionally, there are both fixed and variable O&M costs. Fixed O&M is an annual cost per the power rating of the energy storage system. Variable O&M is a cost based on the amount of energy put through the energy storage for

Table 3.1: Ranges of values of energy storage performance characteristics. These values were drawn from several sources: a **[38]**, b **[19]**, c **[20]**, d **[39]**, e **[37]**, f **[40]**, g **[41]**. *Carbon-enhanced lead-acid batteries' calendar lifetime were assumed to be the same as traditional lead-acid batteries.

	Pb-A	Pb-C	Li-Ion	S-S	V-Redox	Zn-Br	Flywheel	Capacitor
Round Trip Efficiency	80-90%[a,c]	75%[a]	85-100%[a,c]	75-92%[a,c]	65-85%[a,b]	70-75%[a,b]	85-95%[a,d]	85-98%[c]
Cycle life	1,000-2,000[a,b,c]	3,000-20,000[a,e]	4000[a,d]	3,000-4,000[a,e]	5,000-13,000[a,b,d]	2,000-3,000[a,d]	25,000-1,000,000[a,c]	25,000-500,000[a,c]
Calendar life (year)	3-15[b,c,d]	3-15*	8-15[a,b,d]	12-20[b,d]	10-20[b,d]	5-30[b,d]	20[c]	12-20[c,d]
Self-Discharge (%/year)	24-108%[c,d]	52%[e]	36-108%[b,d]	6205-7300%[b,d]	36-108%[b,e]	24-365%[b,d]	7300-36500%[d]	168-14600%[c,d,f]

Table 3.2: The exact values of energy storage performance characteristics used. Values chosen from the range of values found in the literature.

	Pb-A	Pb-C	Li-Ion	S-S	V-Redox	Zn-Br	Flywheel	Capacitor
Round Trip Efficiency	80%	75%	85%	75%	65%	70%	85%	85%
Cycle life	1,000	3,000	4,000	4,000	5,000	2,000	25,000	25,000
Calendar life (year)	6	6	9	14	12	11	20	14
Self-Discharge (%/year)	24%	52%	36%	6205%	36%	24%	7300%	168%

a given time period (one month for this study) [19]. The table of economic values for each energy storage technology is shown in Table 3.3.

Another significant component to this system is the power control system (PCS) which monitors and controls the charging and discharging of the energy storage as well as converting DC to AC electricity. This was assumed to be replaced every 7 years. A basic costing formula was used to cost the PCS [19].

$$PCScost = PCSbase * \left(\frac{Storage\ Power\ Rating(kW)}{1{,}000}\right)^{-0.2} \quad (3.3)$$

To account for inflation of prices, an average inflation rate of 2.47% per year was applied to future transactions. This number was based on the average inflation of the consumer price index for past ten years [42]. The outputs of the model were hourly, including the cash flows. The hourly cash flows were summed into monthly cash flows. Net present value (NPV) was calculated using a discount rate of 10% annually, compounded monthly [43]. The NPV was divided by the total electricity (kWh-AC) consumed in the system lifetime. This gave a uniform value for comparing energy storage technologies in a stand-alone solar PV system. It was assumed that the installation of a solar PV array and the energy storage system would not impose any additional costs for area/land or housing.

Multiple simulations were ran for each energy storage technology at different sizes of the solar PV array. Simulations were ran from 100 kW to 400 kW array in 10 kW increments. This range was chosen because 100 kW is just large enough of an array to produce sufficient energy (although intermittent) for 10 average homes, and 400 kW is rather large, requiring roughly 160 m^2 of crystalline silicon panels on an average Midwest

Table 3.3: Economic factors for the cost of various energy storage technologies. Data from several sources: a **[38]**, b **[19]**, f **[40]**, g **[41]**. *Fixed O&M costs for carbon-enhanced lead-acid batteries were assumed to be the same as those for traditional lead-acid batteries. **Variable O&M costs for supercapacitors were assumed to be negligible.

	Pb-A	Pb-C	Li-Ion	S-S	V-Redox	Zn-Br	Flywheel	Capacitor
Energy Cost ($/kWh)[a]	$330.00	$330.00	$600.00	$350.00	$600.00	$400.00	$1,600.00	$10,000.00
Power Cost ($/kW)[a]	$400.00	$400.00	$400.00	$350.00	$400.00	$400.00	$600.00	$500.00
Fixed O&M Cost ($/kW-year)	$1.55[b]	$1.55*	$0.00[b]	$9.00[b]	$4.00[b]	$0.00[b]	$11.60[g]	$10.00[f]
Variable O&M Cost ($/kWh)	$0.01[b]	$0.01[b]	$0.00[b]	$0.00[b]	$0.00[b]	$0.004[b]	$0.00314[g]	0.00**

roof (assuming 2 stories for the average house) of 102 m^2 and an average Midwest lot of 2,024 m^2 [16] [44] [45]. The PV array size that yielded the lowest NPV/kWh-AC was used as the optimal design for that particular energy storage technology.

3.2.3 Sensitivity Analysis. As will be seen in the results section, the oldest, most developed energy storage technology, lead-acid batteries, were found to have the lowest lifetime costs, with carbon-enhanced lead-acid batteries nearly the same. A simple one-factor-at-a-time (OFAT) sensitivity analysis was done on the 4 performance factors and the 4 economic factors of lead-acid batteries, as well as the solar PV cost. Each factor was either increased or decreased (depending on which would cause a decrease in electricity cost) by factors of 5%, 10%, and 15%. These numbers simulate incremental improvements in energy storage performance or incremental reductions in the various costs examined. The percentage of change in electricity cost (NPV/kWh-AC) from the baseline numbers was recorded (note that NPV/kWh-AC was taken to 6 decimal places). This simple OFAT sensitivity analysis identified the extent to which individual factors affect the overall system costs, but it did not account for higher order interactions.

Additionally, a similar sensitivity analysis was performed on sulfur-sodium batteries. This was because they differ from lead-acid batteries in that they have significantly larger self-discharge. The economic effects of reducing this value were to be examined.

3.3 RESULTS

Table 3.4 shows the key metrics that resulted from the comparison of energy storage technologies. Energy storage size was one main cost driver. The energy storage

size is a function of both self-discharge rate and round-trip efficiency. It can be seen that lithium-ion batteries require the smallest energy storage size due to their excellent performance characteristics. The other major driver of cost was the number of replacements of the energy storage system. The main value to compare the different energy storage technologies was the electricity cost.

Lead-acid batteries performed slightly better than carbon-enhanced lead-acid batteries. Supercapacitors and flywheels produced unrealistic numbers. This was because they are very cost-effective for high power discharges, but have poor energy storage densities and high CapEx. It is important to note that these electricity cost values were calculated using the least optimal values of the ranges of performance parameters with the exception of self-discharge rate.

The results of the sensitivity analysis performed on the base case of each energy storage technology can be found in Tables 3.5-3.12. Graphical representations are seen in Figures 3.2-3.25. There will be one table followed by three figures for each energy storage technology examined in this order: lead-acid battery, carbon-enhanced lead-acid battery, lithium-ion battery, sulfur-sodium battery, vanadium redox battery, zinc bromide battery, flywheel, supercapacitor.

It appears that for 6 out of 8 solar PV-energy storage hybrid systems, incremental changes only 3 of the 9 factors proved to have significant effect on the overall system costs: round-trip efficiency, energy storage costs, and solar PV costs. However, 2 out of 8 solar PV-energy storage hybrid systems additionally saw impact from incremental improvements in self-discharge rate.

Table 3.4: Results from the energy storage technologies comparison. Replacements are energy storage systems required over the 25 year system life in addition to the original installation. The most important value to note is the electricity cost.

	Pb-A	Pb-C	Li-Ion	S-S	V-Redox	Zn-Br	Flywheel	Capacitor
PV Array Storage Size (kW)	320	290	310	400	370	350	400	400
Energy Storage Size (kWh)	1,165	1,613	1,161	1,370	1,181	1,183	1,299	866
Average SOC	88.12%	89.21%	88.26%	83.71%	88.28%	88.29%	86.57%	86.66%
Replacements	4	4	2	1	1	2	1	1
NPV ($1000)	$1,474	$1,522	$1,751	$1,831	$1,963	$1,661	$3,444	$10,020
Electricity Cost (NPV/kWh-AC)	$0.431	$0.443	$0.509	$0.533	$0.571	$0.483	$1.002	$2.914

Table 3.5: Results from the sensitivity analysis of factors for the lead-acid battery. The top parameters were multiplied or divided by a 'factor' from the baseline value. The bottom parameters were varied by increasing percent. The results show the cost of electricity (NPV/kWh) and the percent decrease in cost from the baseline value of $0.428533.

		Percent Change in Factor					
		5%		10%		15%	
	Factors	NPV/kWh	Change (%)	NPV/kWh	Change (%)	NPV/kWh	Change (%)
Energy Storage Performance	Cycle Life	$0.428533	0.000%	$0.428533	0.000%	$0.428533	0.000%
	Calendar Life (year)	$0.428484	-0.011%	$0.428451	-0.019%	$0.428433	-0.023%
	Self-Discharge (%/year)	$0.428523	-0.002%	$0.428513	-0.005%	$0.428502	-0.007%
	Round-Trip Efficiency	$0.418586	-2.321%	$0.409496	-4.442%	$0.400955	-6.435%
Energy Storage Costs	Energy Cost ($/kWh)	$0.422207	-1.476%	$0.414607	-3.250%	$0.407008	-5.023%
	Power Cost ($/kW)	$0.428218	-0.073%	$0.427903	-0.147%	$0.427588	-0.220%
	Fixed O&M ($/kW)	$0.428532	0.000%	$0.428531	0.000%	$0.428530	-0.001%
	Variable O&M ($/kWh)	$0.428521	-0.003%	$0.428509	-0.006%	$0.428498	-0.008%
	Solar PV Cost ($/kW)	$0.413039	-3.616%	$0.397545	-7.231%	$0.382052	-10.847%

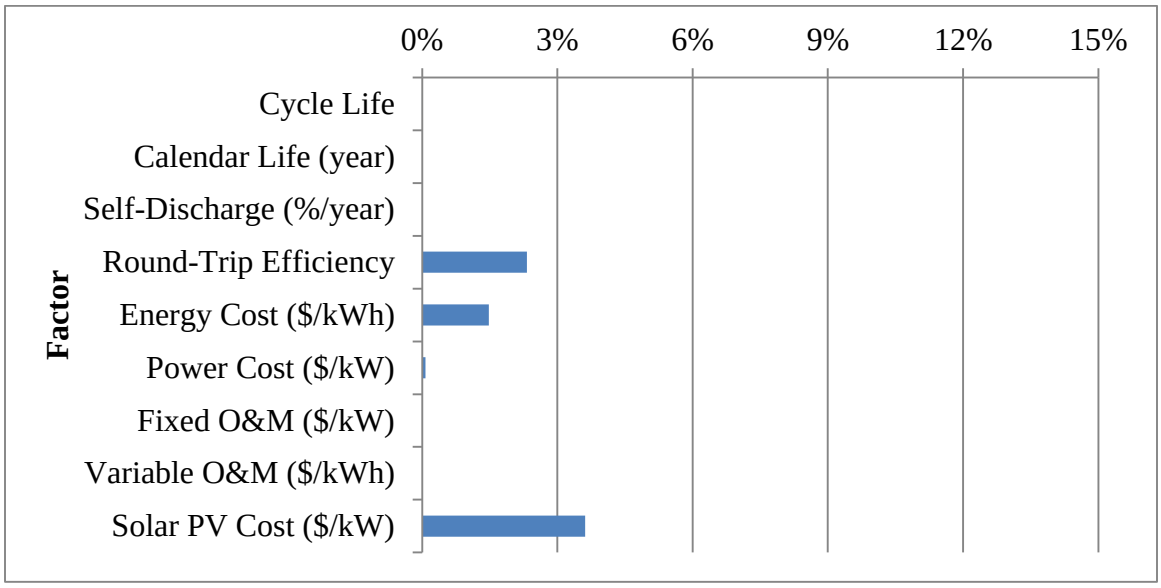

Figure 3.2: Graphical representation of Table 3.5 when modifying factors by 5%. Factors are for the lead-acid battery system.

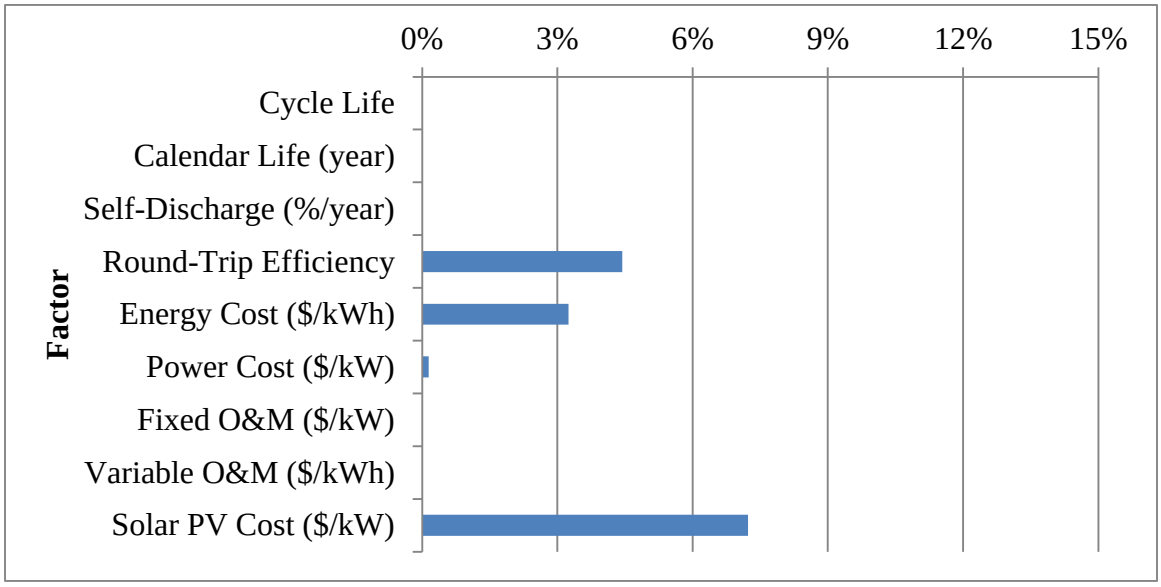

Figure 3.3: Graphical representation of Table 3.5 when modifying factors by 10%. Factors are for the lead-acid battery system.

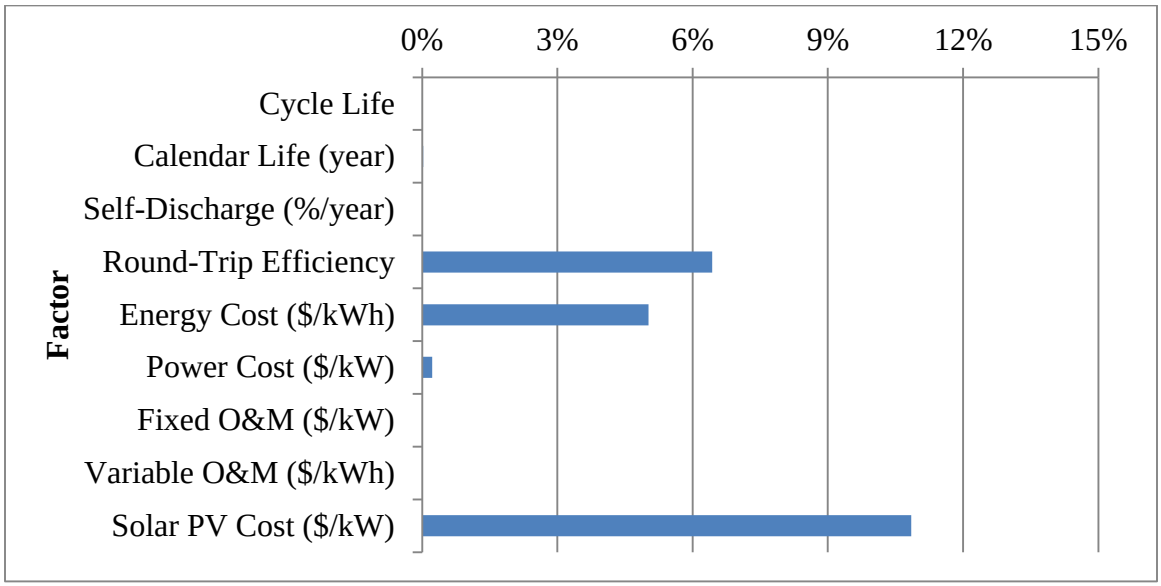

Figure 3.4: Graphical representation of Table 3.5 when modifying factors by 15%. Factors are for the lead-acid battery system.

Table 3.6: Results from the sensitivity analysis of factors for the carbon-enhanced lead-acid battery. The top parameters were multiplied or divided by a 'factor' from the baseline value. The bottom parameters were varied by increasing percent. The results show the cost of electricity (NPV/kWh) and the percent decrease in cost from the baseline value of $0.442509.

		Percent Change in Factor					
		5%		10%		15%	
	Factors	NPV/kWh	Change (%)	NPV/kWh	Change (%)	NPV/kWh	Change (%)
Energy Storage Performance	Cycle Life	$0.442509	0.000%	$0.442509	0.000%	$0.442509	0.000%
	Calendar Life (year)	$0.442442	-0.015%	$0.442397	-0.025%	$0.442372	-0.031%
	Self-Discharge (%/year)	$0.442448	-0.014%	$0.442387	-0.028%	$0.442326	-0.041%
	Round-Trip Efficiency	$0.432305	-2.306%	$0.422289	-4.569%	$0.413187	-6.626%
Energy Storage Costs	Energy Cost ($/kWh)	$0.434758	-1.752%	$0.427008	-3.503%	$0.419257	-5.254%
	Power Cost ($/kW)	$0.442194	-0.071%	$0.441879	-0.142%	$0.441564	-0.214%
	Fixed O&M ($/kW)	$0.442508	0.000%	$0.442507	-0.001%	$0.442506	-0.001%
	Variable O&M ($/kWh)	$0.442497	-0.003%	$0.442485	-0.005%	$0.442473	-0.008%
	Solar PV Cost ($/kW)	$0.427256	-3.447%	$0.411278	-7.058%	$0.395300	-10.668%

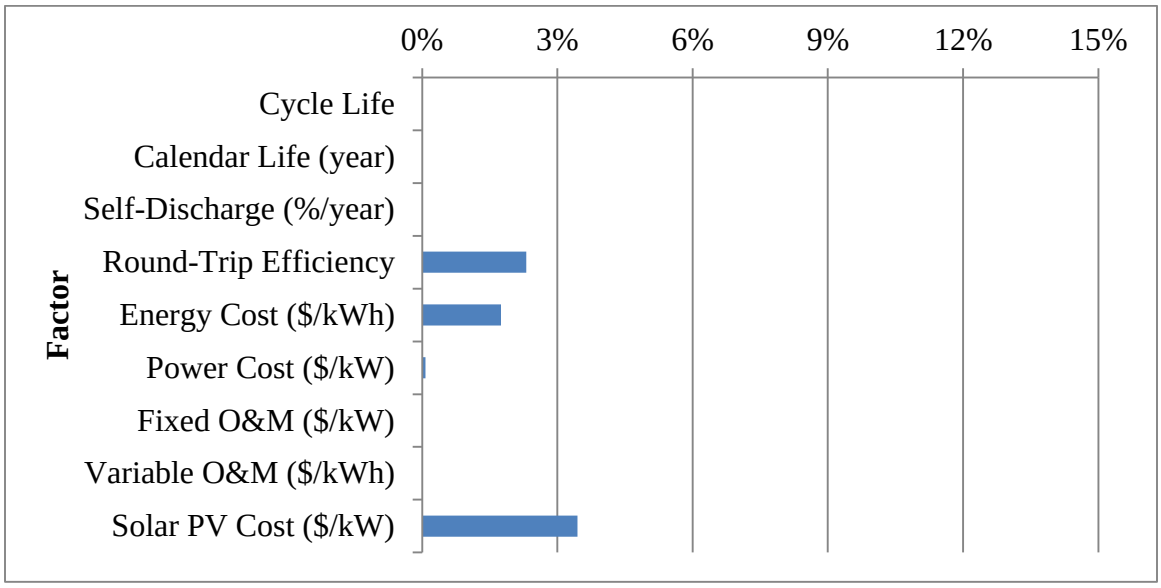

Figure 3.5: Graphical representation of Table 3.6 when modifying factors by 5%. Factors are for the carbon-enhance lead-acid battery system.

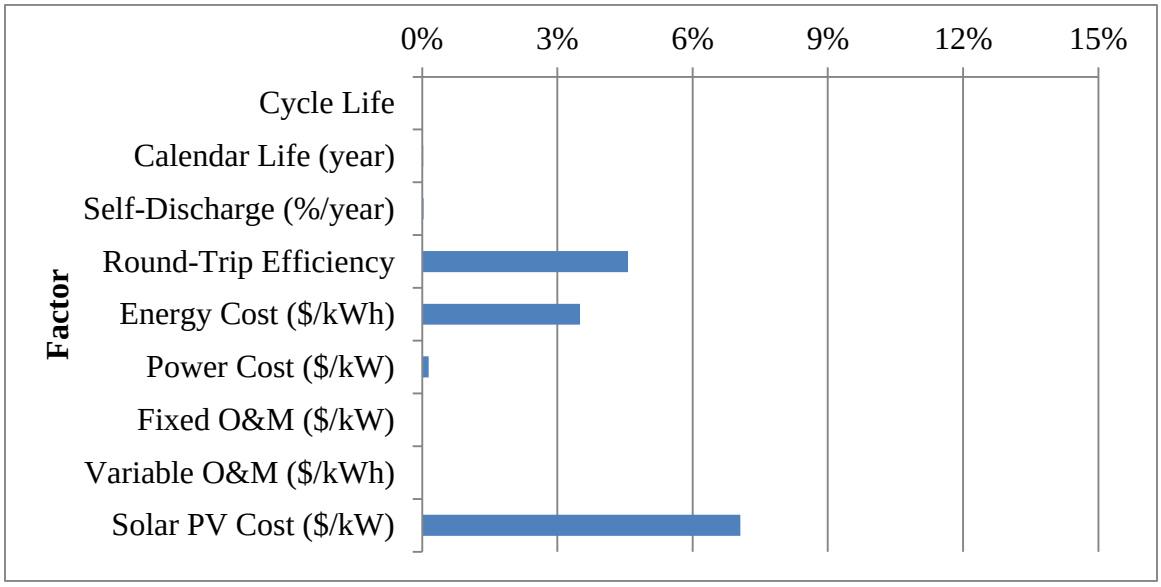

Figure 3.6: Graphical representation of Table 3.6 when modifying factors by 10%. Factors are for the carbon-enhance lead-acid battery system.

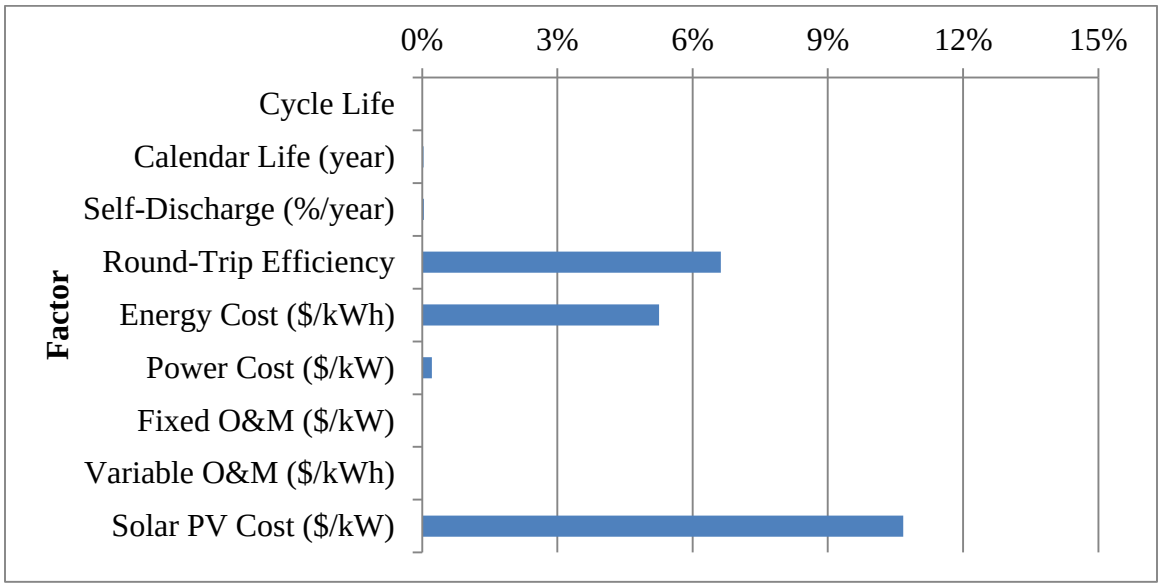

Figure 3.7: Graphical representation of Table 3.6 when modifying factors by 15%. Factors are for the carbon-enhance lead-acid battery system.

Table 3.7: Results from the sensitivity analysis of factors for the lithium-ion battery. The top parameters were multiplied or divided by a 'factor' from the baseline value. The bottom parameters were varied by increasing percent. The results show the cost of electricity (NPV/kWh) and the percent decrease in cost from the baseline value of $0.509203.

		Percent Change in Factor					
		5%		10%		15%	
	Factors	NPV/kWh	Change (%)	NPV/kWh	Change (%)	NPV/kWh	Change (%)
Energy Storage Performance	Cycle Life	$0.509203	0.000%	$0.509203	0.000%	$0.509203	0.000%
	Calendar Life (year)	$0.509199	-0.001%	$0.509197	-0.001%	$0.509195	-0.002%
	Self-Discharge (%/year)	$0.509175	-0.006%	$0.509147	-0.011%	$0.509119	-0.016%
	Round-Trip Efficiency	$0.500168	-1.774%	$0.491691	-3.439%	$0.483775	-4.994%
Energy Storage Costs	Energy Cost ($/kWh)	$0.499073	-1.989%	$0.488943	-3.979%	$0.478812	-5.968%
	Power Cost ($/kW)	$0.508888	-0.062%	$0.508574	-0.124%	$0.508259	-0.185%
	Fixed O&M ($/kW)	$0.509203	0.000%	$0.509203	0.000%	$0.509203	0.000%
	Variable O&M ($/kWh)	$0.509203	0.000%	$0.509203	0.000%	$0.509203	0.000%
	Solar PV Cost ($/kW)	$0.494193	-2.948%	$0.479183	-5.895%	$0.464174	-8.843%

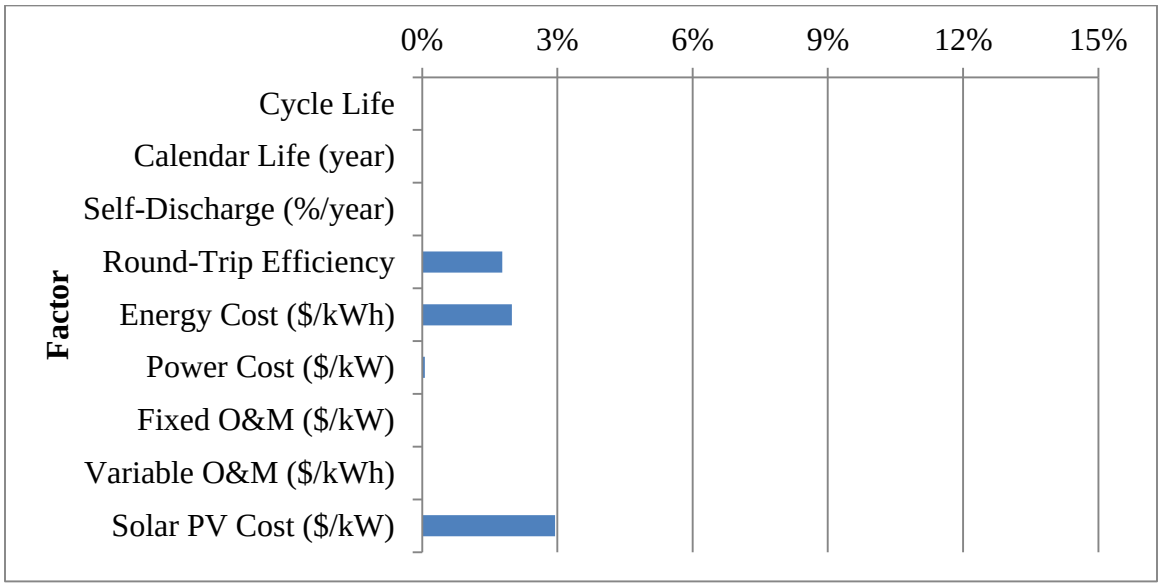

Figure 3.8: Graphical representation of Table 3.7 when modifying factors by 5%. Factors are for the lithium-ion battery system.

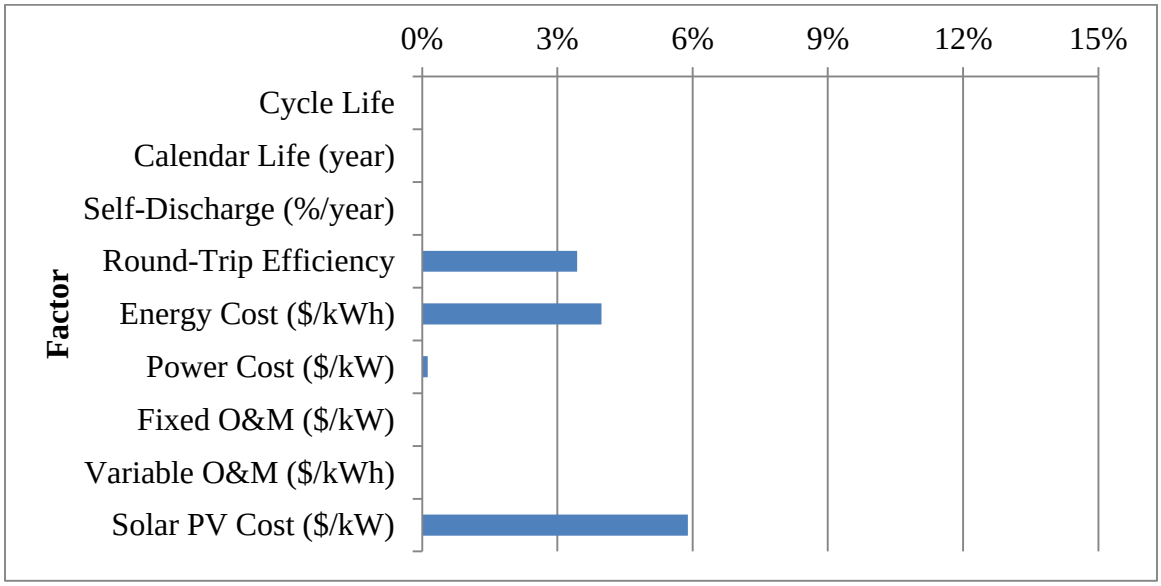

Figure 3.9: Graphical representation of Table 3.7 when modifying factors by 10%. Factors are for the lithium-ion battery system.

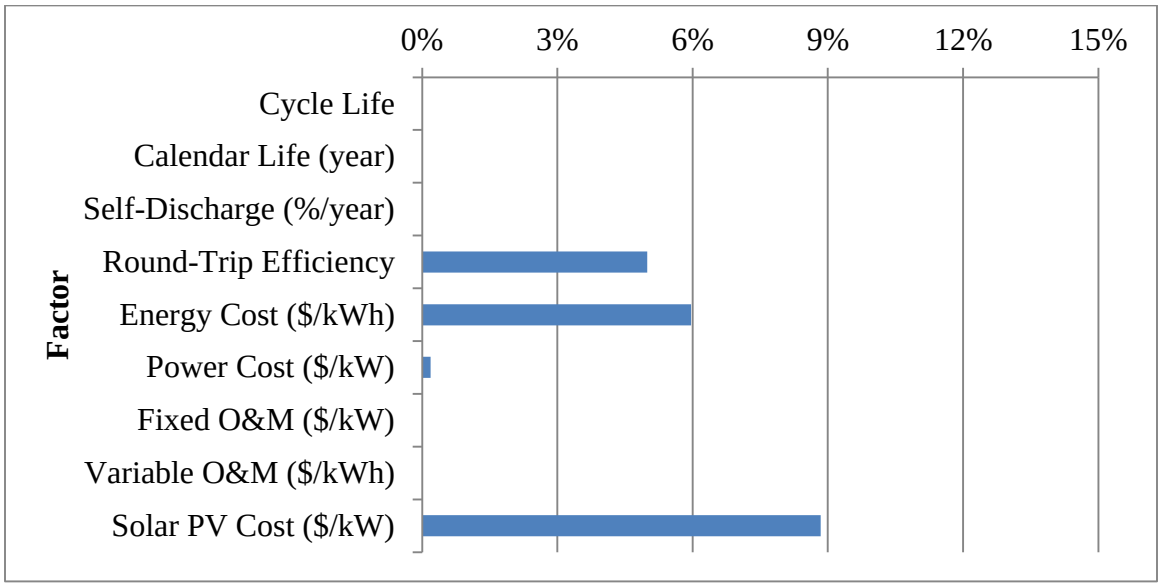

Figure 3.10: Graphical representation of Table 3.7 when modifying factors by 15%. Factors are for the lithium-ion battery system.

Table 3.8: Results from the sensitivity analysis of factors for the sulfur-sodium battery. The top parameters were multiplied or divided by a 'factor' from the baseline value. The bottom parameters were varied by increasing percent. The results show the cost of electricity (NPV/kWh) and the percent decrease in cost from the baseline value of $0.532561.

		Percent Change in Factor					
		5%		10%		15%	
	Factors	NPV/kWh	Change (%)	NPV/kWh	Change (%)	NPV/kWh	Change (%)
Energy Storage Performance	Cycle Life	$0.532561	0.000%	$0.532561	0.000%	$0.532561	0.000%
	Calendar Life (year)	$0.532561	0.000%	$0.532561	0.000%	$0.532561	0.000%
	Self-Discharge (%/year)	$0.527558	-0.939%	$0.522842	-1.825%	$0.515381	-3.226%
	Round-Trip Efficiency	$0.520282	-2.306%	$0.509678	-4.297%	$0.496684	-6.737%
Energy Storage Costs	Energy Cost ($/kWh)	$0.525588	-1.309%	$0.518614	-2.619%	$0.511640	-3.928%
	Power Cost ($/kW)	$0.532286	-0.052%	$0.532011	-0.103%	$0.531736	-0.155%
	Fixed O&M ($/kW)	$0.532555	-0.001%	$0.532549	-0.002%	$0.532543	-0.003%
	Variable O&M ($/kWh)	$0.532561	0.000%	$0.532561	0.000%	$0.532561	0.000%
	Solar PV Cost ($/kW)	$0.513194	-3.637%	$0.493827	-7.273%	$0.474460	-10.910%

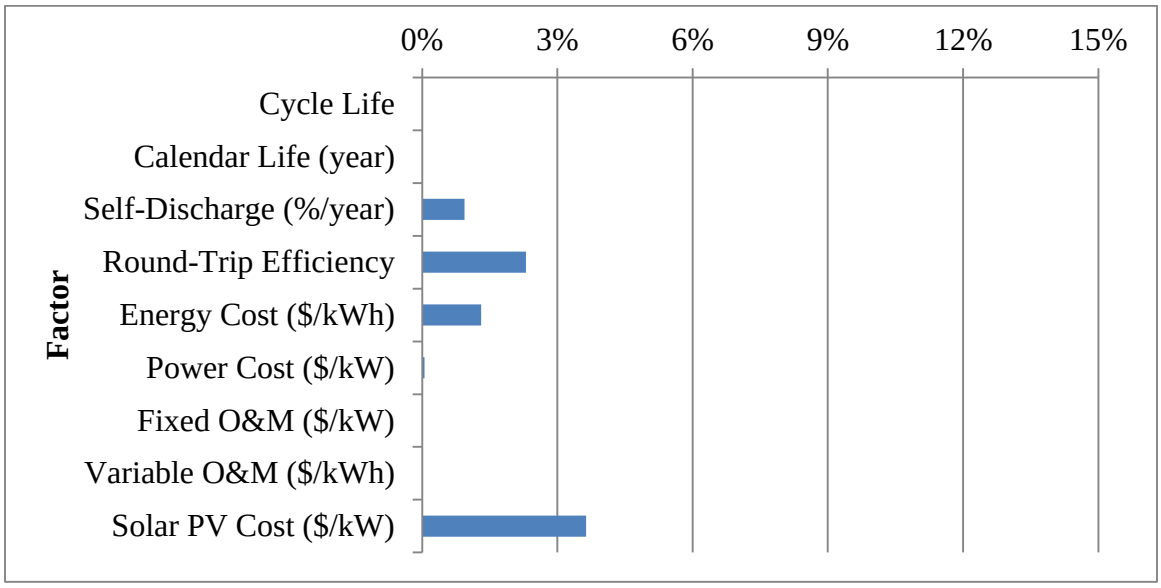

Figure 3.11: Graphical representation of Table 3.8 when modifying factors by 5%. Factors are for the sulfur-sodium battery system.

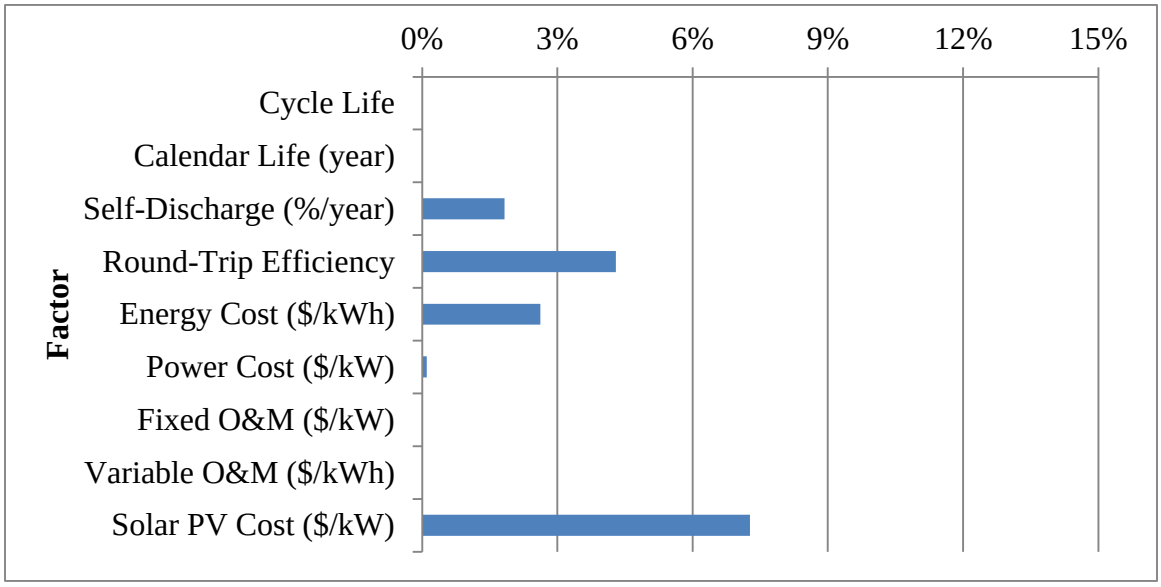

Figure 3.12: Graphical representation of Table 3.8 when modifying factors by 10%. Factors are for the sulfur-sodium battery system.

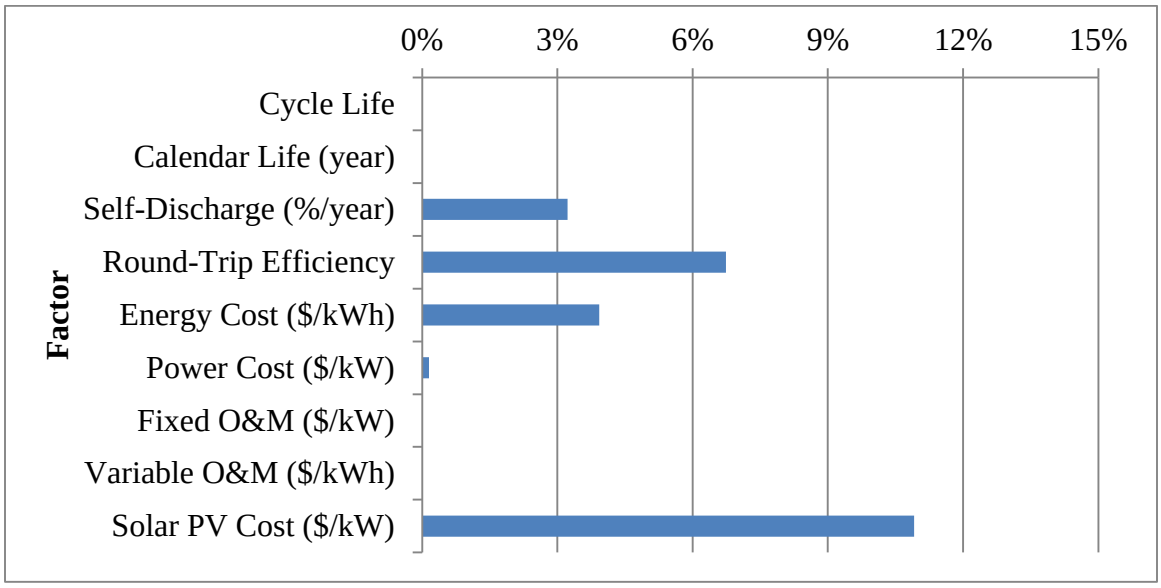

Figure 3.13: Graphical representation of Table 3.8 when modifying factors by 15%. Factors are for the sulfur-sodium battery system.

Table 3.9: Results from the sensitivity analysis of factors for the vanadium redox battery. The top parameters were multiplied or divided by a 'factor' from the baseline value. The bottom parameters were varied by increasing percent. The results show the cost of electricity (NPV/kWh) and the percent decrease in cost from the baseline value of $0.570810.

		Percent Change in Factor					
		5%		10%		15%	
	Factors	NPV/kWh	Change (%)	NPV/kWh	Change (%)	NPV/kWh	Change (%)
Energy Storage Performance	Cycle Life	$0.570810	0.000%	$0.570810	0.000%	$0.570810	0.000%
	Calendar Life (year)	$0.570810	0.000%	$0.570810	0.000%	$0.570810	0.000%
	Self-Discharge (%/year)	$0.570756	-0.009%	$0.570702	-0.019%	$0.570648	-0.028%
	Round-Trip Efficiency	$0.556391	-2.526%	$0.545495	-4.435%	$0.535956	-6.106%
Energy Storage Costs	Energy Cost ($/kWh)	$0.560508	-1.805%	$0.550205	-3.610%	$0.539902	-5.415%
	Power Cost ($/kW)	$0.570496	-0.055%	$0.570181	-0.110%	$0.569867	-0.165%
	Fixed O&M ($/kW)	$0.570808	0.000%	$0.570805	-0.001%	$0.570802	-0.001%
	Variable O&M ($/kWh)	$0.570810	0.000%	$0.570810	0.000%	$0.570810	0.000%
	Solar PV Cost ($/kW)	$0.552560	-3.197%	$0.534161	-6.421%	$0.515762	-9.644%

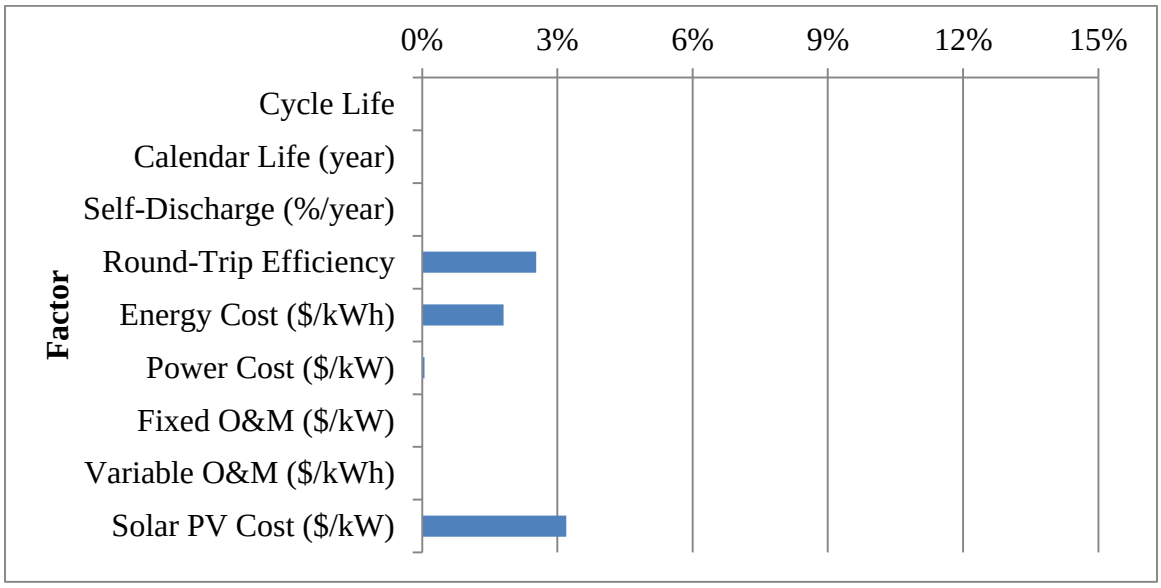

Figure 3.14: Graphical representation of Table 3.9 when modifying factors by 5%. Factors are for the vanadium redox battery system.

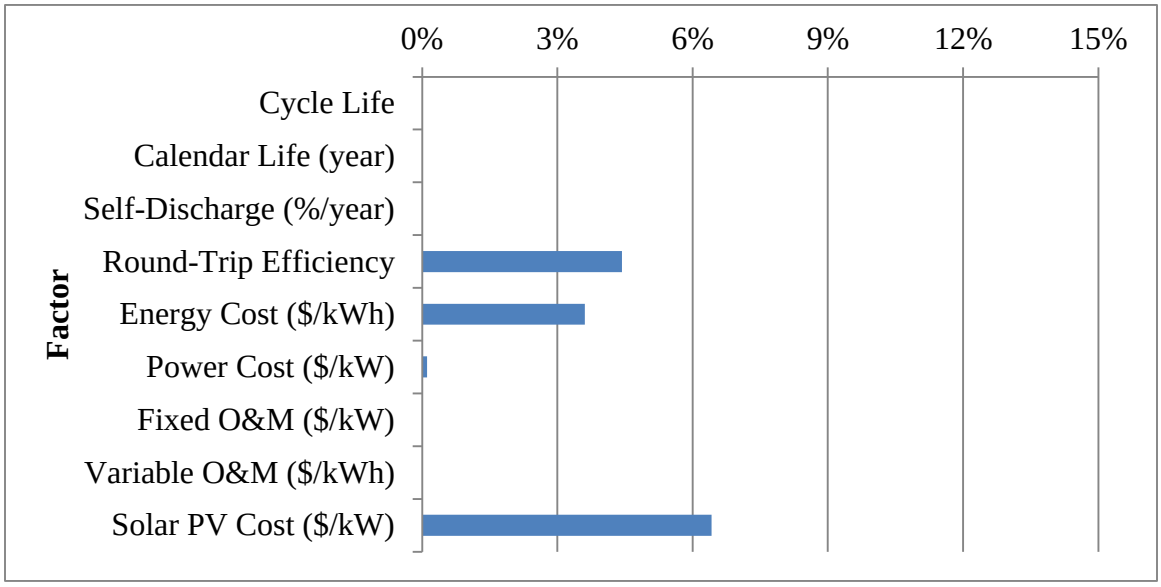

Figure 3.15: Graphical representation of Table 3.9 when modifying factors by 10%. Factors are for the vanadium redox battery system.

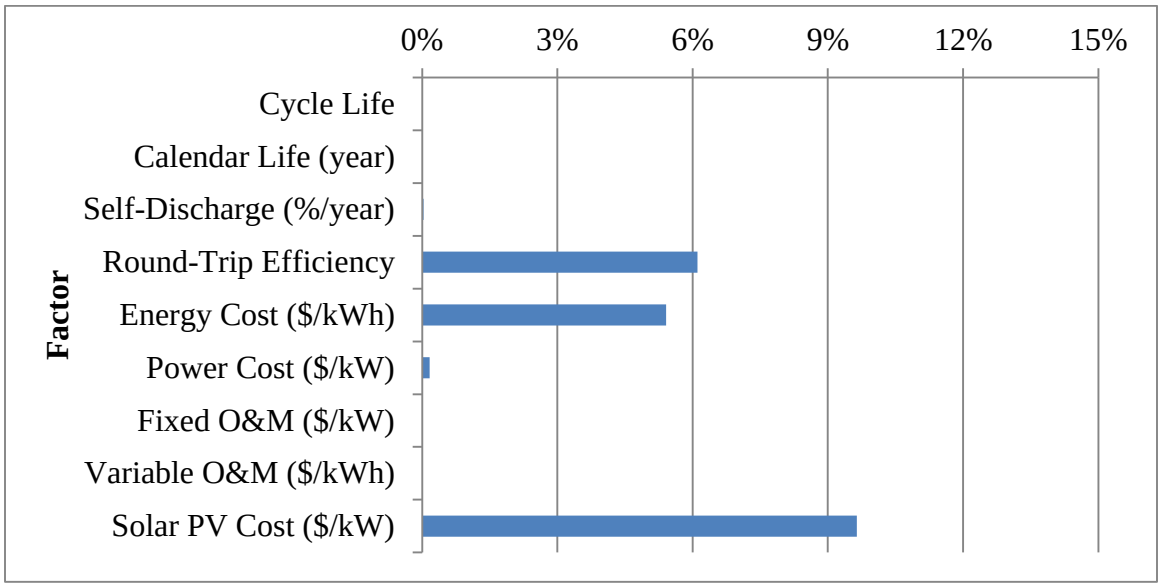

Figure 3.16: Graphical representation of Table 3.9 when modifying factors by 15%. Factors are for the vanadium redox battery system.

Table 3.10: Results from the sensitivity analysis of factors for the zinc bromide battery. The top parameters were multiplied or divided by a 'factor' from the baseline value. The bottom parameters were varied by increasing percent. The results show the cost of electricity (NPV/kWh) and the percent decrease in cost from the baseline value of $0.483053.

		Percent Change in Factor					
		5%		10%		15%	
	Factors	NPV/kWh	Change (%)	NPV/kWh	Change (%)	NPV/kWh	Change (%)
Energy Storage Performance	Cycle Life	$0.483053	0.000%	$0.483053	0.000%	$0.483053	0.000%
	Calendar Life (year)	$0.483052	0.000%	$0.483052	0.000%	$0.483052	0.000%
	Self-Discharge (%/year)	$0.483029	-0.005%	$0.483004	-0.010%	$0.482980	-0.015%
	Round-Trip Efficiency	$0.470970	-2.501%	$0.460774	-4.612%	$0.451484	-6.535%
Energy Storage Costs	Energy Cost ($/kWh)	$0.476172	-1.425%	$0.469134	-2.882%	$0.460109	-4.750%
	Power Cost ($/kW)	$0.482738	-0.065%	$0.482424	-0.130%	$0.482109	-0.195%
	Fixed O&M ($/kW)	$0.483053	0.000%	$0.483053	0.000%	$0.483053	0.000%
	Variable O&M ($/kWh)	$0.483048	-0.001%	$0.483043	-0.002%	$0.483039	-0.003%
	Solar PV Cost ($/kW)	$0.466106	-3.508%	$0.449160	-7.016%	$0.432214	-10.525%

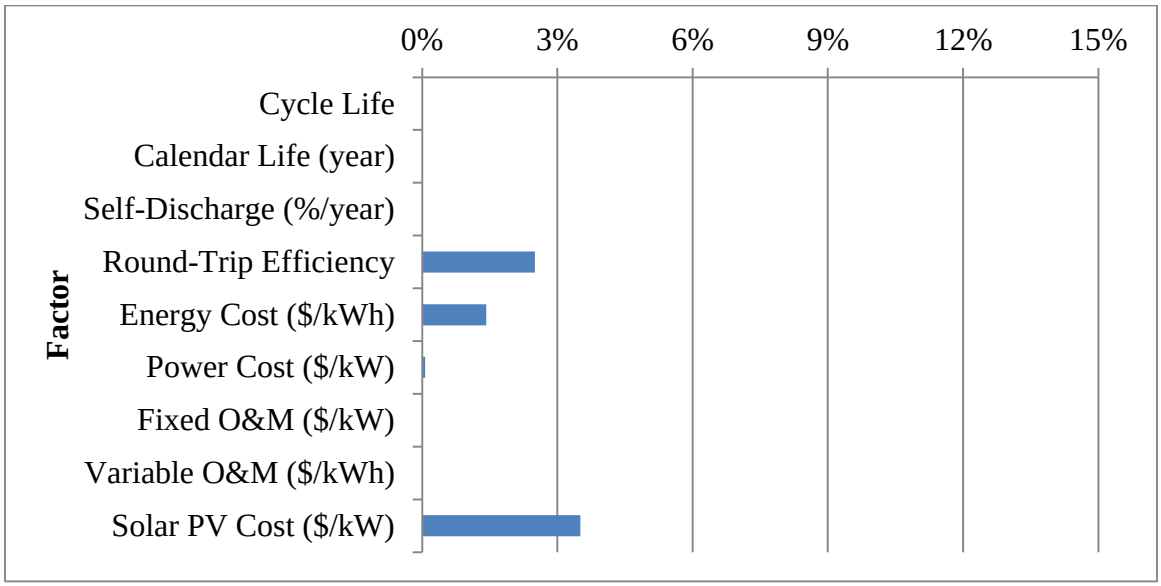

Figure 3.17: Graphical representation of Table 3.10 when modifying factors by 5%. Factors are for the zinc bromide battery system.

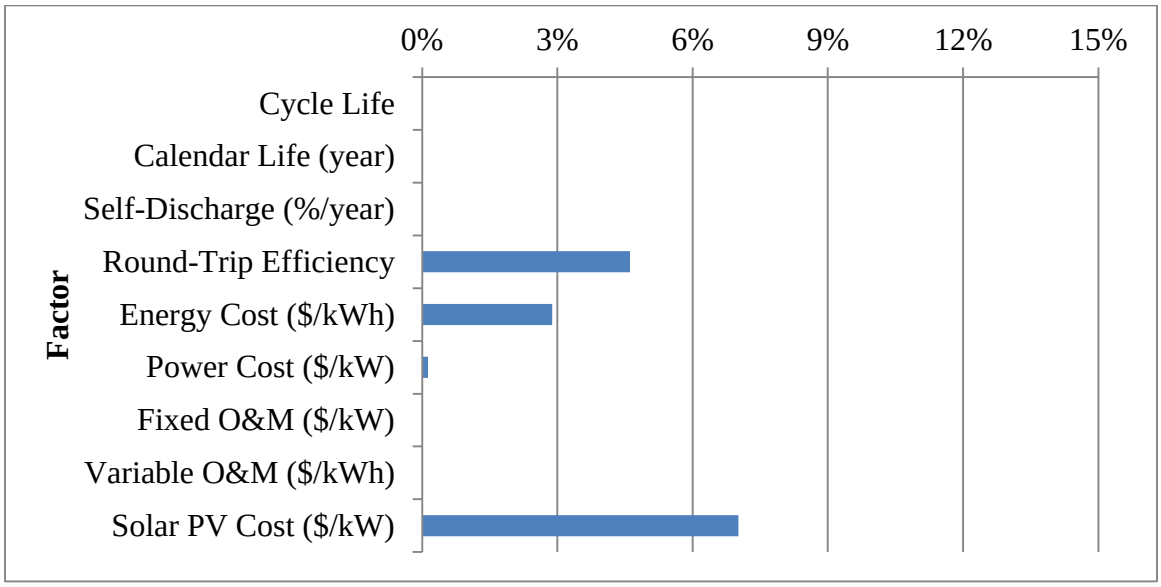

Figure 3.18: Graphical representation of Table 3.10 when modifying factors by 10%. Factors are for the zinc bromide battery system.

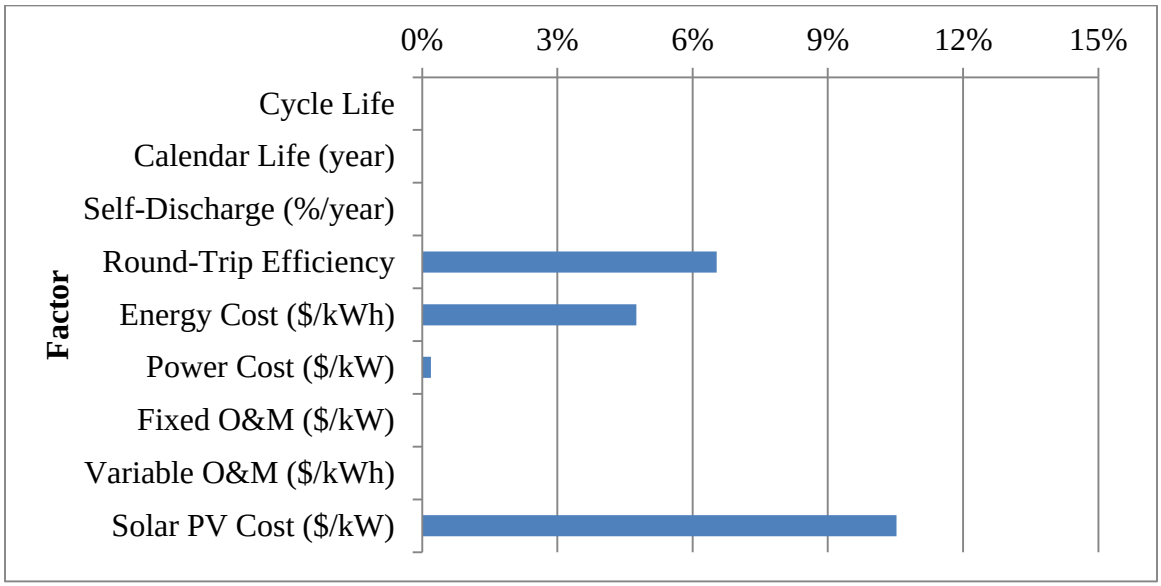

Figure 3.19: Graphical representation of Table 3.10 when modifying factors by 15%. Factors are for the zinc bromide battery system.

Table 3.11: Results from the sensitivity analysis of factors for the flywheel. The top parameters were multiplied or divided by a 'factor' from the baseline value. The bottom parameters were varied by increasing percent. The results show the cost of electricity (NPV/kWh) and the percent decrease in cost from the baseline value of $1.001525.

		Percent Change in Factor					
		5%		10%		15%	
	Factors	NPV/kWh	Change (%)	NPV/kWh	Change (%)	NPV/kWh	Change (%)
Energy Storage Performance	Cycle Life	$1.001525	0.000%	$1.001525	0.000%	$1.001525	0.000%
	Calendar Life (year)	$1.001525	0.000%	$1.001525	0.000%	$1.615322	61.286%
	Self-Discharge (%/year)	$0.982654	-1.884%	$0.964727	-3.674%	$0.947678	-5.376%
	Round-Trip Efficiency	$0.969491	-3.199%	$0.937456	-6.397%	$0.905704	-9.567%
Energy Storage Costs	Energy Cost ($/kWh)	$0.971307	-3.017%	$0.941089	-6.034%	$0.910871	-9.052%
	Power Cost ($/kW)	$1.001054	-0.047%	$1.000582	-0.094%	$1.000110	-0.141%
	Fixed O&M ($/kW)	$1.001518	-0.001%	$1.001510	-0.002%	$1.001502	-0.002%
	Variable O&M ($/kWh)	$1.001520	-0.001%	$1.001514	-0.001%	$1.001509	-0.002%
	Solar PV Cost ($/kW)	$0.982158	-1.934%	$0.962791	-3.868%	$0.943424	-5.801%

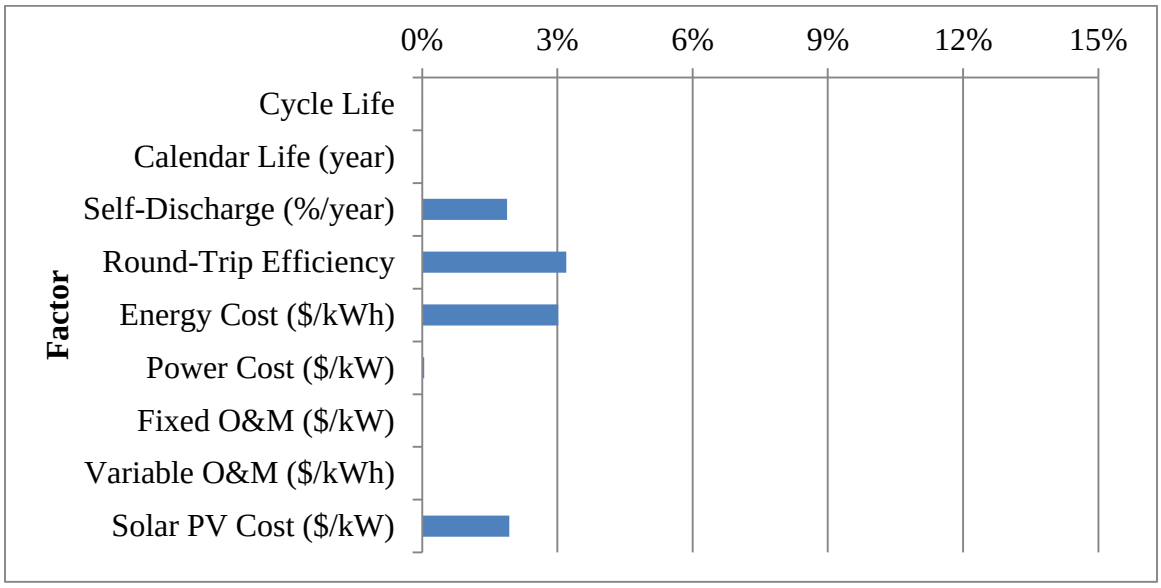

Figure 3.20: Graphical representation of Table 3.11 when modifying factors by 5%. Factors are for the flywheel system.

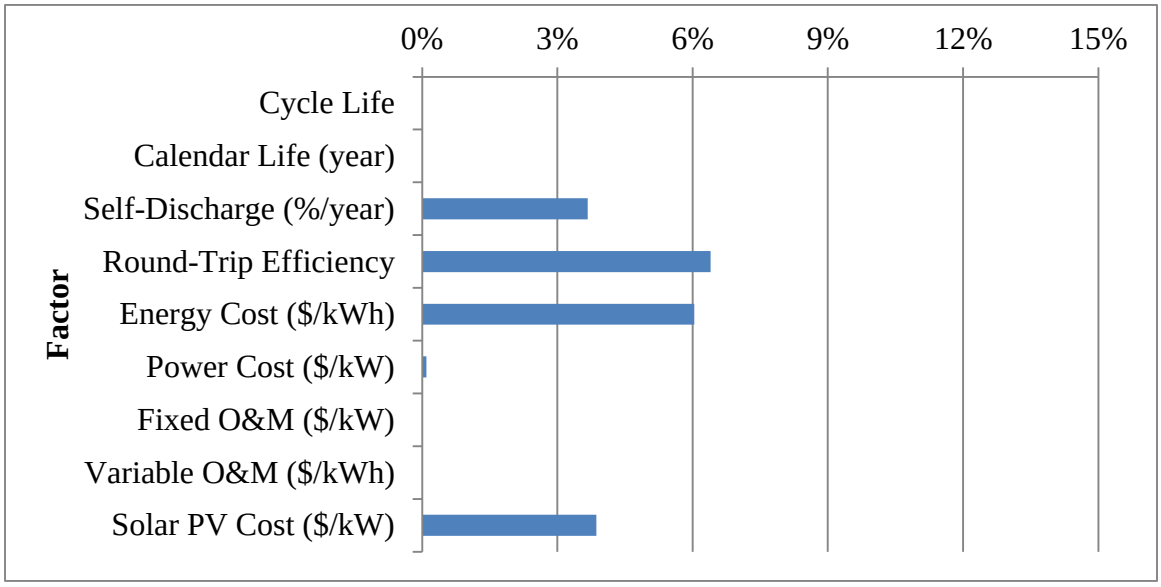

Figure 3.21: Graphical representation of Table 3.11 when modifying factors by 10%. Factors are for the flywheel system.

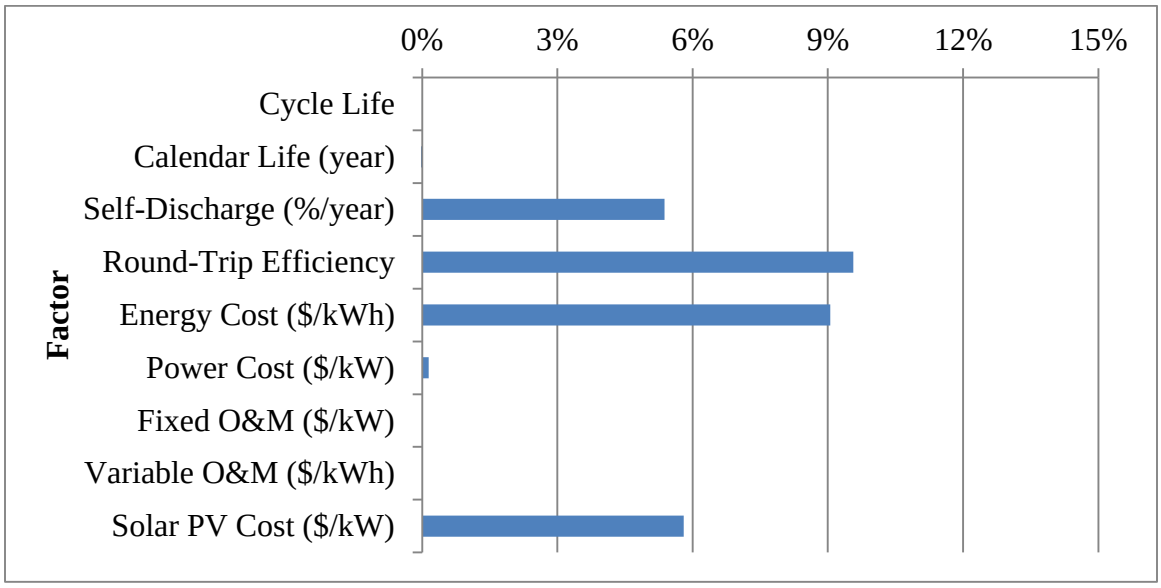

Figure 3.22: Graphical representation of Table 3.11 when modifying factors by 15%. Factors are for the flywheel system.

Table 3.12: Results from the sensitivity analysis of factors for the supercapacitor. The top parameters were multiplied or divided by a 'factor' from the baseline value. The bottom parameters were varied by increasing percent. The results show the cost of electricity (NPV/kWh) and the percent decrease in cost from the baseline value of $2.913869.

		Percent Change in Factor					
		5%		10%		15%	
	Factors	NPV/kWh	Change (%)	NPV/kWh	Change (%)	NPV/kWh	Change (%)
Energy Storage Performance	Cycle Life	$2.913869	0.000%	$2.913869	0.000%	$2.913869	0.000%
	Calendar Life (year)	$2.913869	0.000%	$2.913869	0.000%	$2.913869	0.000%
	Self-Discharge (%/year)	$2.912252	-0.056%	$2.910637	-0.111%	$2.909024	-0.166%
	Round-Trip Efficiency	$2.778730	-4.638%	$2.643591	-9.276%	$2.508452	-13.913%
Energy Storage Costs	Energy Cost ($/kWh)	$2.787949	-4.321%	$2.662028	-8.643%	$2.536108	-12.964%
	Power Cost ($/kW)	$2.913476	-0.014%	$2.913083	-0.027%	$2.912690	-0.040%
	Fixed O&M ($/kW)	$2.913863	0.000%	$2.913856	0.000%	$2.913849	-0.001%
	Variable O&M ($/kWh)	$2.913869	0.000%	$2.913869	0.000%	$2.913869	0.000%
	Solar PV Cost ($/kW)	$2.894502	-0.665%	$2.875135	-1.329%	$2.855768	-1.994%

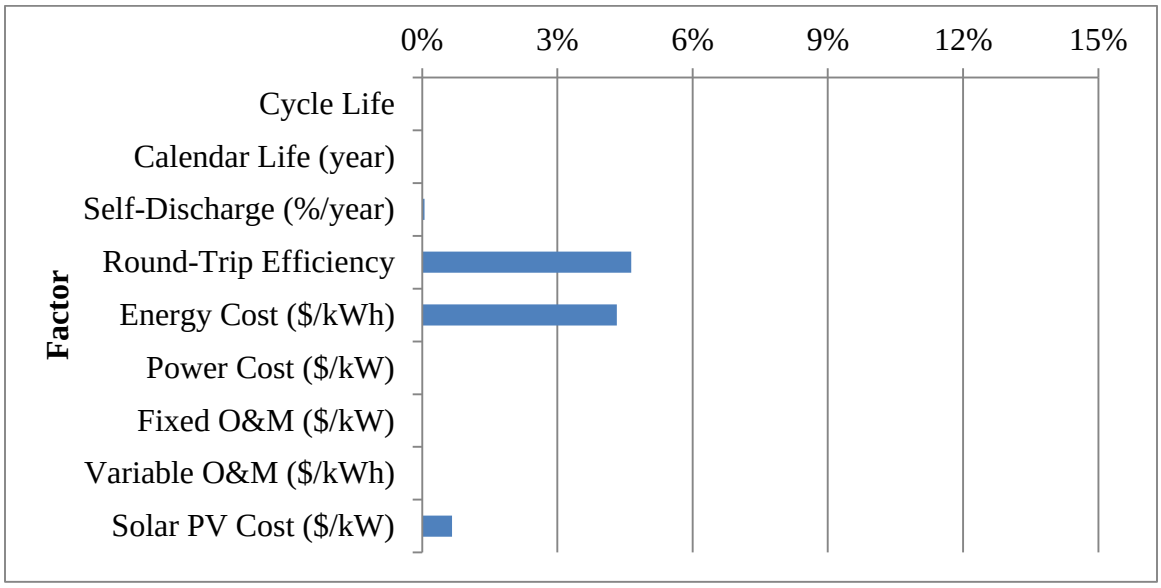

Figure 3.23: Graphical representation of Table 3.12 when modifying factors by 5%. Factors are for the supercapacitor system.

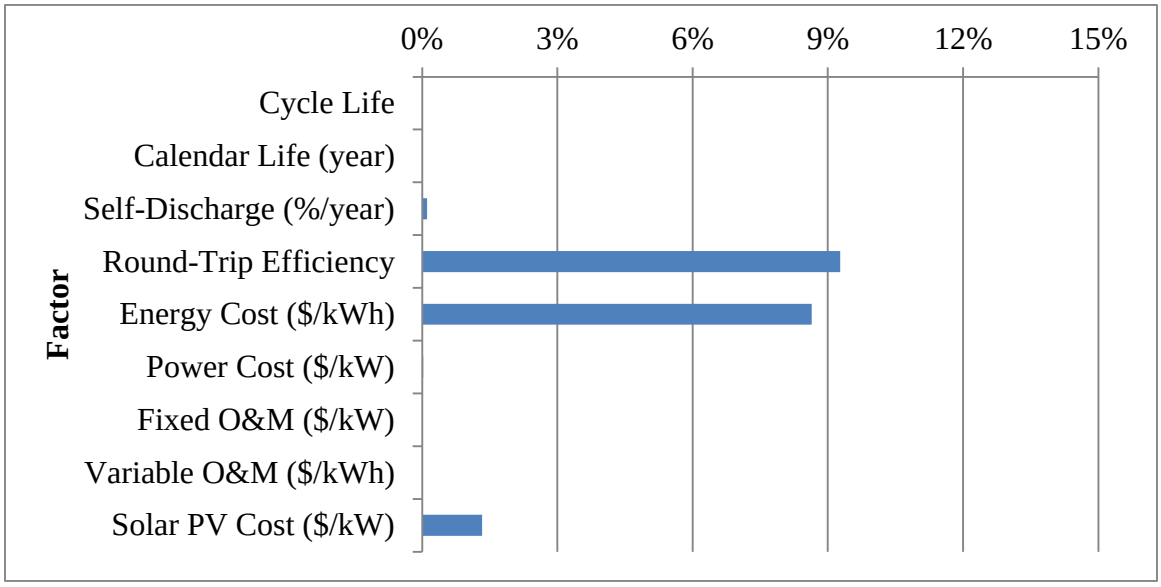

Figure 3.24: Graphical representation of Table 3.12 when modifying factors by 10%. Factors are for the supercapacitor system.

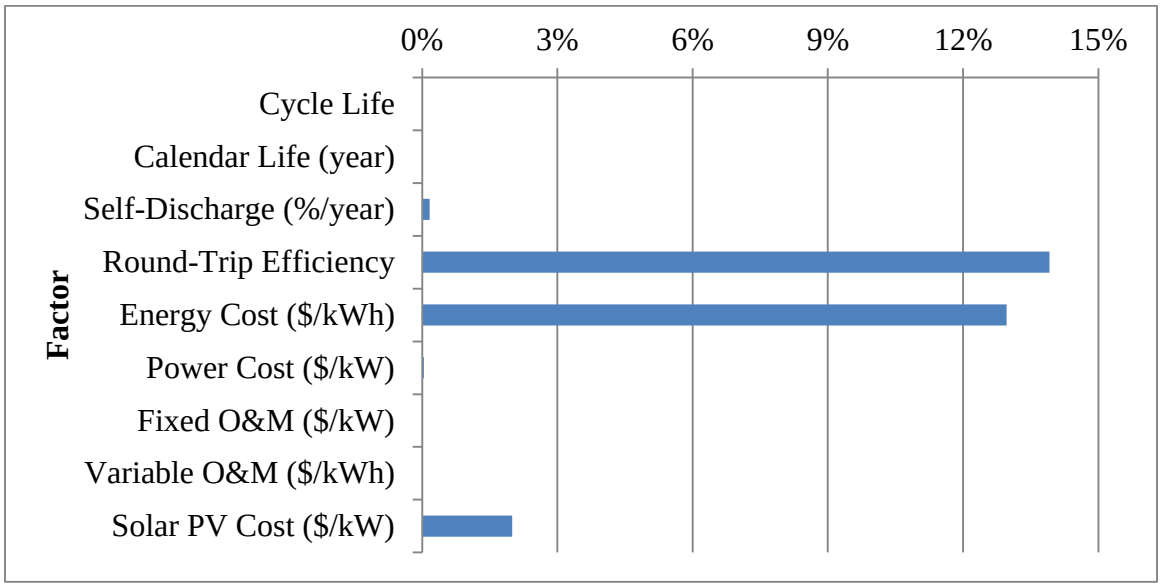

Figure 3.25: Graphical representation of Table 3.12 when modifying factors by 15%. Factors are for the supercapacitor system.

During most of the simulations, calendar lifetime was reached before usage lifetime. This indicated that the throughput lifetime was probably longer than should be expected for most storage technologies, especially electrochemical batteries.

3.4 CONCLUSIONS

Various deployable energy storage options were analyzed for the 25 year lifetime of a stand-alone solar PV and energy storage system sized for 10 average Missouri homes. The results clearly indicate that lead-acid and carbon-enhanced lead-acid batteries provide the best economics. Despite other energy storage technologies that have better performance characteristics, the low cost and reliable nature of lead-based batteries

should still be the first option for economical energy storage in a stand-alone solar PV array.

Simple throughput lifetime modeling appears to be less accurate than what is possible. During the simulations, electrochemical batteries usually reached the calendar lifetime before the throughput lifetime. This is improbable given that the batteries experience deep DOD and frequent PSOC. Future work is discussed later and involves improving usage modeling as a valuable area of potential improvement.

From the sensitivity analysis it was shown that incremental improvement in several factors could lower the cost of the solar PV-energy storage hybrid system. Round-trip efficiency was identified as the most influential energy storage performance factor for improving system costs. Also improvement in self-discharge rate has a significant effect on the system cost for sulfur-sodium batteries and flywheels (energy storage technologies with significantly larger self-discharge rates than the others). On the other hand, incremental improvement in cycle life and calendar life show no significant effects on the overall system costs. Only large improvements in energy storage lifetimes (>>15%) could affect the proposed system's lifetime cost. Energy storage manufacturers and researchers should focus on improving round-trip efficiency and self-discharge rate rather than cycle life and calendar life in order to improve their marketability to the renewable energy market.

These results also show that reducing energy storage cost per kWh has a strong affect as well. From this it can be concluded that energy storage technologies manufacturers and researchers can see similar benefits in focusing their efforts on improving energy storage performance or reducing production costs or both. This is to

say that committing all resources to bettering only energy storage performance or only production costs would be not as wise as a balanced effort in both areas.

Additionally, when designing a stand-alone solar PV and energy storage microgrid, it is important to attempt to maximize the output of the solar PV array, with a panel tilt as close to the ideal tilt for electricity generation (~38° for St. Louis, MO [16]) and an optimal DC to AC derate. This can be done, for instance, by switching from string inverters to micro inverters [17]. This can add to the installed cost of the solar PV, but this cost is negligible compared to the lifetime economics of the system. Trivially, solar PV manufacturers should continue to reduce costs as they have in recent years to increase the adoptability of their product in grid isolated systems coupled with energy storage.

4. LIFE-CYCLE EMMISSIONS ANALYSIS

4.1 INTRODUCTION

Renewable energy will play an important role in the energy future of the world. The success of intermittent wind and solar energy is certainly tied to future advancements and cost reductions in energy storage. Energy storage developments will allow for renewable energy to be integrated into the grid in a more stable fashion as well as enhance the viability of decentralized microgrids and distributed renewable energy generation. Section 3 discussed a comparative life cycle economic analysis of multiple deployable energy storage technologies as used in a grid-isolated solar PV array. Lead-acid batteries and the evolving carbon-enhanced lead-acid batteries show the most promise as economically viable energy storage technologies.

Economics is not the only consideration in the renewable energy-energy storage field. In fact economics is hardly a driving force at all. The interest in renewable energy is primarily one of environmental concerns over fossil fuel emissions, especially carbon dioxide. Presently, renewable energy is not cost competitive with fossil fuel generation, but renewable energy theoretically has less environmental impact than traditional electricity in terms of GHG and other emissions.

This thesis will expand upon the results in Section 3 and compare the life cycle emissions of the three most mature electrochemical batteries studied (lead-acid, lithium-ion, sulfur-sodium). The emissions of the different 10 average Missouri home solar PV-battery storage hybrid microgrids will be compared against each other as well as against typical grid generation represented by coal-fired power plants. Multiple pollutants, CO_2,

NO_x, SO_x, and heavy metals, were considered, but carbon dioxide is of the most interest given the current scientific and political environment with regards to global climate change.

4.2 METHODOLOGY

The results from Section 3 include the cost-optimal size of solar PV (kW), size of energy storage (kWh), and number of energy storage replacements for the three batteries examined. Cradle-to-gate pollution data for CO_2, NO_x, SO_x, and heavy metals (Pb, Cd, Ni, Hg, Cr, As, etc.) were found for crystalline silicon solar PV cells, lead-acid, lithium-ion, and sulfur-sodium batteries (except heavy metal data for lithium-ion and sulfur-sodium).

Pollution data for crystalline silicon solar PV was given in terms of mass per kilowatt-hour electricity generated, assuming 1,700 kWh/m^2-yr for 30 years. The data was back calculated to give pollution data in units of mass per m^2. The pollution data can be found in Table 4.1 [46].

Table 4.1: Cradle-to-gate pollution data for solar PV. Data given per surface area of crystalline silicon solar PV **[46]**.

Pollutant	CO_2 (kg/m^2)	NO_x (g/m^2)	SO_x (g/m^2)	HM (mg/m^2)
	2,550	8,976	17,595	1,224

Pollution data for electrochemical batteries was given in terms of mass pollutant per mass of battery. In order to define the life cycle pollution data in mass per kilowatt-hour battery capacity, specific energy numbers were needed. It was assumed that for this 10-home microgrid batteries would be selected to maximize energy capacity rather than power capacity. For this reason, the higher values for specific energy were used in calculating mass pollutant per kWh capacity. Table 4.2 contains the original pollutant data in terms of mass per mass, the specific energy ranges of the three batteries, the maximum value in the specific energy range used, and the final mass pollutant per kWh that was used to complete this analysis [47] [39].

Table 4.2: Pollution data for various electrochemical battery chemistries. Data given per mass of battery, specific energy ranges for the batteries, value of specific energy used for conversion to pollution per kWh basis, and the new pollution data per kWh of battery capacity **[47] [39]**.

Battery Chemistry		Lead-Acid	Lithium-Ion	Sulfur-Sodium
Original Pollutant Data	CO_2 (kg/kg)	3.2	12.5	13.3
	NO_x (g/kg)	4.6	14.5	16
	SO_x (g/kg)	7	19.7	29.3
	HM (mg/kg)	215	N/A	N/A
Specific Energy Range (kWh/kg)		0.03-0.05	0.1-0.25	0.15-0.24
Specific Energy Used (kWh/kg)		0.05	0.25	0.24
Modified Pollutant Data	CO_2 (kg/kWh)	62	50	55.4
	NO_x (g/kWh)	92	58	66.7
	SO_x (g/kWh)	140	78.8	122.1
	HM (mg/kWh)	4300	N/A	N/A

From Section 3, the size of the solar array was initially defined in kW installed capacity. It was assumed that the crystalline silicon solar PV modules would have 0.25 kW capacity per m^2. The solar PV pollutant data and the PV area were multiplied to give the total pollution contribution from the solar array. Battery pollution data was multiplied by the battery energy storage size (kWh). This number was then multiplied by the number of replacements plus one to account for all battery-related pollution over the entire system lifetime. These figures were then also divided by the total kWh of AC electricity consumed over the system lifetime. This pollution per kWh was compared to values traditionally associated with crystalline solar PV and with pollution from traditional fossil fuel electricity generation.

4.3 RESULTS

The results for the full solar PV-battery storage system lifetime cradle-to-gate pollution can be found Table 4.3, Table 4.4, and Table 4.5 for lead-acid, lithium-ion, and sulfur-sodium batteries, respectively. Note that the most economical configuration in terms of solar PV size and energy storage size and replacements from Section 3 were used.

The results show that within the basis of the 10 average Missouri home microgrid, lithium-ion batteries with solar PV show the lowest emissions for the gaseous pollutants, CO_2, NO_x, and SO_x. Lithium-ion batteries also proved to produce the lowest heavy metal pollution, although this number was skewed because there were no comparable cradle-to-gate heavy metal pollution data for either lithium-ion or sulfur-sodium batteries.

Table 4.3: Results of the cradle-to-gate pollution analysis for lead-acid batteries. Batteries were coupled with a solar photovoltaic array. Analysis was done using the most feasible system from Section 3.

Solar PV Size: 320 kW/1280 m^2				Energy Storage Size: 1165 kWh			
Total Pollution				Pollution per kWh Consumed			
	Solar PV	Storage	Total		Solar PV	Storage	Total
MM kg CO_2	3.264	0.373	3.637	kg CO_2/kWh	0.949	0.109	1.058
MM g NO_x	11.489	0.535	12.025	g NO_x/kWh	3.341	0.156	3.497
MM g SO_x	22.521	0.466	22.989	g SO_x/kWh	6.549	0.135	6.684
MM mg HM	1.567	25.042	26.609	mg HM/kWh	0.456	7.282	7.737

Table 4.4: Results of the cradle-to-gate pollution analysis for lithium-ion batteries. Batteries were coupled with a solar photovoltaic array. Analysis was done using the most feasible system from Section 3.

Solar PV Size: 310 kW/1240 m^2				Energy Storage Size: 1161 kWh			
Total Pollution				Pollution per kWh Consumed			
	Solar PV	Storage	Total		Solar PV	Storage	Total
MM kg CO_2	3.162	0.174	3.336	kg CO_2/kWh	0.920	0.051	0.970
MM g NO_x	11.130	0.202	11.332	g NO_x/kWh	3.237	0.059	3.295
MM g SO_x	21.818	0.274	22.092	g SO_x/kWh	6.345	0.080	6.425
MM mg HM	1.518	N/A	1.518*	mg HM/kWh	0.441	N/A	0.441*

Table 4.5: Results of the cradle-to-gate pollution analysis for sulfur-sodium batteries. Batteries were coupled with a solar photovoltaic array. Analysis was done using the most feasible system from Section 3.

Solar PV Size: 400 kW/1600 m^2				Energy Storage Size: 1370 kWh			
Total Pollution				Pollution per kWh Consumed			
	Solar PV	Storage	Total		Solar PV	Storage	Total
MM kg CO_2	4.080	0.152	4.232	kg CO_2/kWh	1.187	0.044	1.231
MM g NO_x	14.362	0.183	14.545	g NO_x/kWh	4.176	0.053	4.229
MM g SO_x	28.152	0.334	28.486	g SO_x/kWh	8.187	0.097	8.284
MM mg HM	1.958	N/A	1.958*	mg HM/kWh	0.569	N/A	0.569*

The results also show that sulfur-sodium batteries actually have the worst emissions of the gaseous pollutants examined. This is mostly a result of the large size of sulfur-sodium energy storage needed.

A recent NREL publication on life cycle GHG emissions for solar PV stated that CO_2 pollution was only around 40 g CO_2 eq/kWh. Coal generation produced around 1,000 g CO_2 eq/kWh [48] [49] [50]. The solar PV component of CO_2 emissions for the lithium-ion battery system, the "cleanest" system, showed 920 g/kWh. There was a vast discrepancy between the numbers found in this study and the number published by NREL. This was because the NREL data assumed a grid-connected solar PV system where all electric generation was either used directly by the local demand, or excess generation was transmitted to wider grid use. For a grid-isolated system, not all electricity generated by the solar PV is used. When the array is out-producing demand and energy storage is "filled" to capacity, electricity must be shunted to prevent overcharging of energy storage. The results of this study were calculated based on kWh of AC electricity consumed by the 10 average homes.

4.4 CONCLUSION

When comparing lead-acid, lithium-ion, and sulfur-sodium electrochemical battery storage technologies coupled with a solar PV array to meet average residential electricity needs, lithium-ion batteries show the lowest levels of CO_2, NO_x, SO_x, and heavy metals (Pb, Cd, Ni, Hg, Cr, As, etc.) emissions. Of course the comparable cradle-to-gate data of heavy metals for lithium-ion and sulfur-sodium was not present, but lead-acid batteries do tend to involve heavy metals (obviously, lead) to a large degree.

Carbon dioxide emissions are often the most concerning form of pollution at least as of this writing. Solar PV coupled with lithium-ion batteries produced less carbon dioxide than the NREL estimates for emissions from coal-fired electricity generation. The system with lead-acid batteries is competitive with the coal electricity carbon dioxide production. It is important to note that for the three cases, the major portion of the gaseous emissions is produced from the solar PV life cycle as opposed to the energy storage life cycle. It is interesting that this was the case considering that the calculation performed to determine emissions/kWh only accounted for AC kWh's consumed. The solar PV produced at least double the energy as what would be required to strictly meet the residential demand assuming no cost or self-discharge or round-trip inefficiencies with energy storage.

Overall, grid-isolated solar PV and battery storage systems can be pollution-competitive with the existing fossil-fuel generated electricity in terms of carbon dioxide emissions. This conclusion comes from calculations based on a scenario that is far from an ideal utilization of renewable energy. More efficient usage (possibly through further hybridization) of the solar PV electricity would improve the pollution efficiency.

5. CONCLUSION AND SUMMARY

5.1 CONCLUSIONS

Adopting renewable energy sources such as wind and solar is a growing concern globally as atmospheric carbon dioxide levels continue to rise and fossil fuel reserves continue to deplete. The intermittent nature of renewable energy dictates that the development of energy storage technology is crucial to the increase in renewable energy footprint. There is a very wide range of technologies available for storing energy, each having its own advantages, disadvantages, and room for improvement. Understanding the differences between energy storage technologies and how they interact with renewable energy is critical to determining the best technological approaches for today and the future.

This thesis proposed studying energy storage technologies using the basis of a grid-isolated crystalline silicon solar PV system. A uniform approach to modeling the lifetime performance of vastly different energy storage technologies was implemented. This was achieved by using NREL modeling of solar PV output, average electricity consumer data, and using several sources of empirical data for energy storage performance. The study was to cover the estimated 25 year lifetime of the combined solar-storage system.

Section 3 analyzed the life-cycle economic costs of the various solar PV-energy storage systems. This was performed by using a throughput counting method to determine replacement times for the energy storage technology. Initial capital costs, replacement capital costs, and O&M costs were summed into monthly cash flows, and

the NPV per kilowatt-hour AC electricity consumed was calculated as the economic comparison tool. Lead-acid batteries still showed the lowest life-cycle costs for stationary, non-space-limited scenarios. They were closely followed by the promising and developing carbon-enhanced lead-acid batteries. High-performing lithium-ion batteries have prohibitive capital costs and have shown difficulty in being implemented in large-scale settings. Other technologies show promise as they mature including sulfur-sodium and flow batteries. High-speed flywheels and supercapacitors are the furthest from cost viability in energy storage as they have high capital costs, high self-discharge rates, and low energy densities. They appear best suited for power quality applications rather than energy storage.

From a simple OFAT sensitivity analysis of the model some conclusions were drawn. For all the energy storage technologies, incremental improvements in the energy storage performance parameter of round-trip efficiency had significant impact on the cost of the overall systems studied in Section 3. Additionally, incremental improvement in self-discharge rate had a significant impact on the overall system cost for sulfur-sodium batteries and flywheels, the two technologies with significantly higher self-discharge rates. However, incremental improvements in cycle life and calendar life show little effect in alter system lifetime costs. Only significant increases in energy storage lifetime (>>15%) could impact the overall system costs. Also, reducing costs of producing energy storage technologies has comparable impact compared to improving energy storage performance parameters. This indicates that energy storage technology manufacturers and researchers can be most effective in improving their products' marketability in stand-

alone solar PV systems by looking to improve their technology's round-trip efficiency and self-discharge while at the same time aiming to reduce production costs.

Section 4 studied the environmental impact of the electrochemical battery-solar PV systems studied in Section 3. Lithium-ion batteries proved to be the lowest emissions in all of the areas studied: CO_2, NO_x, SO_x, and heavy metals. Both lead-acid and lithium-ion batteries combined with solar PV produced less carbon dioxide per kWh AC consumed when compared to coal-generated electricity. Sulfur-sodium batteries showed the most pollution. This is due to the necessary size of the sulfur-sodium battery because of its high self-discharge rate.

The throughput counting model used to estimate storage lifetime was probably too liberal in that the energy storage systems, even electrochemical batteries, were reaching their calendar life limits rather than their throughput usage limits during most simulations. Factors for both DOD and maintaining a PSOC are needed for each different energy storage technology to improve accuracy.

It appears that presently, lead-acid batteries still offer the best energy storage technology when combining economic and environmental factors. Although developing carbon-enhanced lead-acid batteries may over-take their cousins in the very near future.

5.2 RECOMMENDED FUTURE WORK

There are a lot of areas where this research can be improved, expanded, and/or validated. Energy storage should remain a research area of focus globally and for Missouri S&T. Below are some recommendations of related areas to further explore:

1. Other energy sources can be added to the model. Wind generation would be the most logical in continuation of the renewable energy theme. This would probably require data more granular than on an hourly basis.
2. The solar and/or energy storage modeling could be incorporated into other hybrid energy systems currently being researched within Missouri S&T's ERDC.
3. Improvements should be made on the lifetime modeling of the energy storage systems. This can be done by adding additional parameters to the throughput counting method or exploring other methods.
4. Modeling for solar PV-energy storage systems should be verified by physical experimentation. From this further modeling inferences and improvements can be made.
5. An analysis of optimization of the solar PV-energy storage hybrid microgrid's composition should be performed:
    a. One approach could be one of purely analyzing the economy of scale for the system.
    b. Another approach could be how to optimize the demographics of the microgrid's inhabitants in order to minimize demand variability.
6. A full supply chain analysis from raw material to finished product of each energy storage technology should be performed. This assessment would include a product price and availability outlook for both the short- and long-term.

5.3 CONCLUDING REMARKS

- Energy storage is immensely important in the current and future energy infrastructure as renewable energy plays an increasing role.
- Various energy storage technologies are very different, but each has potential to be important in specific areas of interest.
- Continued improvement in the performance and production costs of energy storage technologies will directly correlate to the growth of solar and wind technologies for central, distributed, and grid-isolated electricity generation.
- Improving the modeling of energy storage will enhance the economic and environmental visibility for future applications.

APPENDIX

The following is the Matlab code used for the modeling in this thesis. Input parameters for the energy storage are for lead-acid batteries in this example. There is a main code with 3 subroutines, 2 will be listed after the main code; the third is a trivial code to calculate NPV when given cash flows and discount rate per compounding period are given (function name “pvvar”) and will be omitted.

In Matlab coding, commentary is separated from the code by lines beginning with a “%” symbol. Code can be sectioned off by commentary lines beginning with the “%%” symbol. Lines of code that actually execute commands end with a “;”. Note that the text of the code wraps to the next line in some instances, making it difficult to differentiate code from commentary. The main function called “primary_model” consists of 9 sections. The first 5 sections are for inputting different classes of data. The final 4 sections perform calculations and call subroutine codes which are shown after the “primary_model” code. The sections of “primary_model” in order of execution are as follows:

- %%Input solar PV generation
- %%Input demand data
- %%Energy storage performance parameters
- %%Costing and economic data
- %%Pollution data
- %%Size energy storage (calls “energy_size” subroutine)
- %%Estimate storage lifetime (calls “battery_lifetime” subroutine)

- %%Run economic analysis (calls “pvvar” subroutine, code not listed)
- %%Pollution analysis

Below is the beginning of the main code, “primary_model”:

```
function primary_model()

%% Input solar PV generation

% Define location to call PVWatts data
location='St. Louis, MO';

% Define fixed solar PV tilt (zenith: 0 degrees--flat panel, 90
% degrees--vertical panel) and compass direction (azimuth: 0 north, 90
% east, 180 south, 270 west). These values are used to call PVWatts data
panel_zenith=15;
panel_azimuth=180;

% Define derate in converting from DC to AC. This is used to define PVWatts
% data
derate=0.87;

% Convert PVWatts-data-defining parameters to strings and multiply derate
% by 100
panel_zenith=num2str(panel_zenith);
panel_azimuth=num2str(panel_azimuth);
derate_str=num2str(derate*100);

% Store relevant PVWatts data. Note the data is for 25 years or 219,000
% hours. Also note that this data is in watts per 100 kW rated capacity of
% solar PV
generation=xlsread(strcat(location, ',', panel_zenith, ',', panel_azimuth, ',', derate_str,
'.xlsx'),'A1:A219000');

% Define total hours in system lifetime and create an hours index array and
% similarly create those for months
hours=size(generation,1);
hour_index=[1:hours]';
months=ceil(hours/730.484);
months_index=[1:months]';

% Define array rated capacity (kW)
```

```
array_capacity=100;

% Define capacity per module (kW) and area per module (m^2) in order to
% calculate the total area (m^2) of the area
capacity_per_module=0.25;
area_per_module=1;
area=array_capacity*area_per_module/capacity_per_module;

% Define the rate at which the solar PV will degrade as a percent of rated
% capacity lost per year
degrade=0.005;

% Generation data is converted from watts to kilowatts, prorated from 100
% kW to the defined array capacity, and modified for degradation at each
% hour. Also rename it as supplyAC
supplyAC=generation/1000/100*array_capacity.*(1-degrade/8760*(hour_index-1));

%% Input demand data

% Define the hourly demand data file to be called
demand_type='Ameren Missouri x 10';

% Store AC demand data
demandAC=xlsread(strcat(demand_type, '.xlsx'),'A2:A219001');

% Define annual AC electricity consumption increase as a percent
consumption_increase=-0.002;

% Account for consumption increase by hour
demandAC=demandAC.*(1+consumption_increase/8760*(hour_index-1));

% Create a DC demand array
demandDC=demandAC/derate;

%% Energy storage performance parameters

% Name storage technology
StorageSelection='Traditional Lead Acid';

% Is the charge rate limited or not? Electrochemical batteries usually have
% limited charge rates which is assumed to be the same as the maximum
% discharge rate. yes=1, no=0.
%limited_charge=1;

% Define the roundtrip efficiency as a percent:
rt_efficiency=0.80;
```

```
% Define the self-discharge of the energy storage as a percent of stored
% capacity lost per year
selfdischarge=.24;

%Define cycle lifetime
cycle_life=1000;

%Define calendar lifetime (years)
calendar_life=6;

% Define maximum allowable depth of discharge as a percent
maxDOD=0.80;

%% Costing and economic data

% Define cost of solar PV (%/kW installed capacity)
cost_per_kW=3330;

%Define energy storage cost (per kWh)
storage_cost_per_kWh=330;

%Define power storage cost (per kW max rating)
storage_cost_per_kW=400;

% Define fixed and variable O&M costs ($/kW-yr and %$/kWh, respectively)
% for energy storage
OMfixed=1.55;%$/kW-yr
OMvariable=0.01;%$/kWh

% Define base for Moshers formula in "Economic Valuation of Energy Storage
% Coupled with Photovoltaics" for costing the Power Control System (PCS)
% and the estimated replacement time in years
PCSbase=230;
PCSreplace=7;

% Define the expected inflation rate and the discount rate for calculating
% present value
inflation=0.0247;
rate=0.10;

%% Pollution data

% Define the pollution per m^2 of solar PV for CO2 (kg), NOx (g), SOx (g),
% and Heavy Metals (mg)
CO2_per_m2=2550;
```

```
NOx_per_m2=8976;
SOx_per_m2=17595;
HM_per_m2=1224;

% Define energy storage specific density (kWh/kg) which will be used for
% calculated storage pollution
energy_density=0.05;

% Define the pollution per kWh of energy storage for CO2 (kg), NOx (g), SOx
% (g), and Heavy Metals (mg)
CO2_per_kWh=3.2/energy_density;
NOx_per_kWh=4.6/energy_density;
SOx_per_kWh=4/energy_density;
HM_per_kWh=215/energy_density;

%% Size energy storage

% Calculate the hourly energy surplus/deficit (kWh)
energy_surplus=(supplyAC-demandAC)/derate;

% Maximum power sizing for energy storage by multiplying maximum DC hourly
% power demand by hourly "power factor" to estimate maximum momentary power
% within the maximum hourly average power:
% ~1.5 for residential
% ~>2.0 for commercial
% ~>2.5 for industrial
% greater numbers indicate larger estimates of overall storage
% power capacity
power_factor=1.5;
power_storage_size=max(demandDC)*power_factor;

% Initial sizing assuming no (0) self discharge with (0) as initial energy
% storage size
[energy_storage_size_old,SOC,SOCpercent,discharge]=storage_size(hours,0,0,rt_efficien
cy,energy_surplus,maxDOD);

% Iterative sizing increasing by 5% until minimum depth of discharge is not
% violated
iter=0;
max_iter=13;
check=999;
while check>1&&iter<max_iter

[energy_storage_size_new,SOC,SOCpercent,charge,discharge]=storage_size(hours,selfdi
scharge,energy_storage_size_old,rt_efficiency,energy_surplus,maxDOD);
    check=abs(energy_storage_size_new-energy_storage_size_old);
```

```
    energy_storage_size_old=energy_storage_size_new;
    iter=iter+1;
end
energy_storage_size=energy_storage_size_old;

% Calculate average state of charge (SOC) percent
avgSOC=mean(SOCpercent);

%% Estimate storage lifetime

% Define throughput life
throughput_life=cycle_life*maxDOD*energy_storage_size;

% Energy storage replacements and "battery life" calculation
[replacements,replacement_hours,battery_life]=battery_lifetime(hours,throughput_life,de
mandDC,selfdischarge,energy_storage_size,energy_surplus,SOCpercent,calendar_life,dis
charge);

% Store total energy storage replacements as a single value
storage_replacements=max(replacement_hours(:,1));

%% Run economic analysis

% Initialize array of monthly cash flows (+1 for month "0")
total_costs=zeros(months+1,1);

% Calculate PV array cost
array_cost=cost_per_kW*array_capacity;

% Calculate energy storage cost based on both the energy storage cost
% component and the power storage cost component
energy_storage_cost=storage_cost_per_kWh*energy_storage_size;
power_storage_cost=storage_cost_per_kW*power_storage_size;

% Calculate PCS cost based on Mosher's formula "Economic
% Valuation of Energy Storage Coupled with Photovoltaics"
PCScost=PCSbase*(power_storage_size/1000)^-0.2;

% Sum initial costs of system in the master cash flow array
total_costs(1)=-(array_cost+energy_storage_cost+power_storage_cost+PCScost);

% Convert PCS replacement time from years to months
PCSmonths=PCSreplace*12;

% Convert storate replacement times from hours to months
replacement_months=replacement_hours;
```

```
replacement_months(:,2)=floor(replacement_hours(:,2)/730.484);

% Add storage replacement costs to the appropriate monthly cash flows
for i=1:size(replacement_months,1)
   total_costs(replacement_months(i,2)+1)=total_costs(replacement_months(i,2)+1)-
(energy_storage_cost+power_storage_cost);
end

% Initialize monthly consumption (kWh)
monthlyconsumption=zeros(months+1,1);

% Add storage fixed O&M, variable O&M, and PCS replacement costs to monthly
% cash flows
for i=2:months+1
   total_costs(i)=total_costs(i)-
OMfixed*power_storage_size/12+OMvariable*sum(discharge((i-2)*730+1:(i-1)*730));
   if mod(i,PCSmonths)==0
      total_costs(i)=total_costs(i)-PCScost;
   end
   monthlyconsumption(i)=sum(demandAC((i-2)*730+1:(i-1)*730));
end

% Account for inflation in cash flows
total_costs(2:months+1)=total_costs(2:months+1).*(1+inflation/12*(months_index-1));

% Calculate present value of all negative cash flows (costs) and present
% value of system per kWh AC consumed
pvcosts=pvvar(total_costs,rate);
costperkwh=pvcosts/sum(demandAC);

%% Perform pollution analysis

% Create array of emission values per m^2 photovoltaic surface area
PVpollution_per_m2=[CO2_per_m2; NOx_per_m2; SOx_per_m2; HM_per_m2];

% Multiply pollution per m^2 values by area (m^2) of solar PV to calculate
% total emissions from solar PV and find the total emissions per kWh AC
% consumed
PVpollution=area*PVpollution_per_m2;
PVpollution_per_kWh_consumed=PVpollution/sum(demandAC);

% Create array of emission values per kWh energy storage
STOREpollution_per_kWh=[CO2_per_kWh; NOx_per_kWh; SOx_per_kWh;
HM_per_kWh];

% Multiply pollution per kWh values by energy storage size to calculate
```

```
% total emissions from energy storage and find the total emissions per kWh
% AC consumed
STOREpollution=energy_storage_size*(1+storage_replacements)*STOREpollution_per_
kWh;
STOREpollution_per_kWh_consumed=STOREpollution/sum(demandAC);

% Calculate total pollution (PV and Storage) and pollution per kWh
pollution=PVpollution+STOREpollution;
pollution_per_kWh=pollution/sum(demandAC);
```

The following is the storage sizing subroutine, “storage_size”, which is utilized in the “%%Energy storage sizing” section of the main code, “primary_model”:

```
function
[energy_storage_size,SOC,SOCpercent,charge,discharge]=storage_size(hours,selfdischar
ge,energy_storage_size,rt_efficiency,energy_surplus,maxDOD)

% Initialize the state of charge (SOC), self-discharge (SD), charge,
% discharge arrays
SOC=zeros(hours,1);
SD=zeros(hours,1);
charge=zeros(hours,1);
discharge=zeros(hours,1);

% Add or subtract energy surplus/deficits at all hours, but this is done
% backwards (sort of). All SOC values are non-positive
if energy_surplus(1,1)>0
   SOC(1,1)=0;
else
   SOC(1,1)=energy_surplus(1,1)+0;
   discharge(1)=energy_surplus(1,1);
end
for i=2:hours
   % Energy storage size must be calculated as an absolute value of the
   % minimal SOC value in order to calculate selfdischarge
   if abs(SOC(i-1,1))>energy_storage_size*maxDOD
      energy_storage_size=abs(SOC(i-1,1))/maxDOD;
   end
   % Self-discharge is calculated by adding energy storage size (positive)
   % to the non-positive SOC to create a non-negative storage capacity to
   % multiply the self-discharge rate
   SD(i-1,1)=(SOC(i-1,1)+energy_storage_size)*selfdischarge/8760;
   SD(i-1,1)=abs(SD(i-1,1));
   % Both charges/discharges and self-discharge are added to the previous
```

```
    % SOC to determine the current SOC
    if energy_surplus(i,1)>0
        charge(i)=-SD(i-1,1)+energy_surplus(i,1)*rt_efficiency;
        SOC(i,1)=SOC(i-1,1)+charge(i);
        if charge(i)<0
            discharge(i)=charge(i);
            charge(i)=0;
        end
    else
        discharge(i)=-SD(i-1,1)+energy_surplus(i,1);
        SOC(i,1)=SOC(i-1,1)+discharge(i);
    end
    % SOC cannot exceed 0. This is the same as saying the storage cannot
    % exceed its maximum capacity
    if SOC(i,1)>0
        charge(i)=abs(SOC(i-1,1));
        SOC(i,1)=0;
    end
end

% SOC values are converted to postive values based on the energey storage
% size and percent state of charge is calculated
SOC=SOC+energy_storage_size;
SOCpercent=SOC/energy_storage_size;
```

The following is the subroutine for calculating storage lifetime based on throughput life and calendar life, called “battery_lifetime”. Note that “battery” is often used in the code variables, this can mean any storage, battery or otherwise. This subroutine is called by the “%%Estimate storage lifetime” section of the main code, “primary_model”:

```
function
[replacements,replacement_hours,battery_life,discharge]=battery_lifetime(hours,through
put_life,demandDC,selfdischarge,energy_storage_size,energy_surplus,SOCpercent,calen
dar_life)

% Initialize the hourly storage discharges, hourly battery life, initial
```

```
% battery life (100%) and initial number of storage replacements beyond
% initial system construction (0)
discharge=zeros(hours,1);
battery_life=zeros(hours,1);
battery_life(1,1)=1.00;
replacements=0;

% n x 2 matrix: 1st column is nth relacement, 2nd column is the hour of the
% nth replacement
replacement_hours=zeros(1,2);

for i=2:hours

   % Storage life is reduced by the percent of throughput in that hour per
   % throughput lifetime
   battery_life(i,1)=battery_life(i-1,1)-demandDC(i)/throughput_life-
selfdischarge/8760*SOCpercent(i)*energy_storage_size/throughput_life;

   % Storage discharge at each hour is recorded
   if energy_surplus(i,1)<0
      discharge(i,1)=energy_surplus(i,1)-
selfdischarge/8760*SOCpercent(i)*energy_storage_size;
   elseif energy_surplus(i,1)>=0
      discharge(i,1)=-selfdischarge/8760*SOCpercent(i)*energy_storage_size;
   end

   % Storage replacement occures either if throughput life reaches 0 or
   % calendar life is reached, with the exception of if only 10% of one
   % calendar life remains in the 25 year life of the system, then it will
   % not be replaced. The number and time of replacements are recorded
   if (battery_life(i,1)<=0||i-
max(replacement_hours(:,2))>=8760*calendar_life)&&hours-i>0.1*8760*calendar_life
      battery_life(i,1)=1.00;
      replacements=replacements+1;
      replacement_hours(replacements,1)=replacements;
      replacement_hours(replacements,2)=i;
   end
end
```

BIBLIOGRAPHY

[1] U.S. Energy Information Administration, "Electricity Net Generation: Total (All Sectors)," U.S. Energy Information Administration, 2013.

[2] U.S. Energy Information Administration, "Energy Outlook 2013," U.S. Department of Energy, 2013.

[3] P. Denholm, E. Ela, B. Kirby and M. Milligan, "The Role of Energy Storage with Renewable Electricity Generation," National Renewable Energy Laboratory, Golden, CO, 2012.

[4] J. Wang, J. D. Wojcik and Y. Zue, *Studyof Supercritical Coal Fired Power Plant Dynamic Responses and Control for Grid Code Compliance*, University of Warwick, 2012.

[5] J. Baker, "New technology and possible advances in energy storage," *Elsevier Energy Policy*, no. 36, pp. 4368-4373, 2008.

[6] C. Richter, "Solar Thermal Energy, Introduction," in *Solar Energy*, Springer, 2013, p. 655.

[7] D. Lincot, "Photovoltaic Energy, Introduction," in *Solar Energy*, Springer, 2013, p. 170.

[8] S. Martinuzzi, A. Slaoui, J.-P. Kleider, M. Lemiti, C. Trassy, C. Levy-Clement, S. Dubois, R. Monna, Y. Veschetti, I. Perichaud, N. L. Quang and J. Kraiem, "Silicon Solar Cells, Crystalline," in *Solar Enegy*, Springer, 2013, p. 226.

[9] G. Stapleton and S. Neill, Grid-Connected Solar Electric Systems, New York, NY: Earthscan, 2012.

[10] C. R. Wronski and N. Wyrsch, "Silicon Solar Cells, Thin-film," in *Solar Energy*, Springer, 2013, p. 270.

[11] S. Buecheler, L. Kranz, J. Perrenoud and A. N. Tiwari, "CdTe Solar Cells," in *Solar Energy*, Springer, 2013, p. 1.

[12] H.-W. Schock, "Solar Cells, Chalcoprite-Based Thin Film," in *Solar Energy*, Springer, 2013, p. 323.

[13] E. D. Glowacki, N. S. Sariciftci and C. W. Tank, "Organic Solar Cells," in *Solar Energy*, Springer, 2013, p. 97.

[14] M. Gratzel, "Mesoscopic Solar Cells," in *Solar Energy*, Springer, 2013, p. 79.

[15] M. Raugei and P. Frankl, "Lif cycle impacts and costs of photovoltaic systems: Current state of the art and future outlooks," *Elsevier Energy,* no. 34, pp. 392-399, 2009.

[16] S. O'Rourke, Interviewee, *VP Consulting Services Microgrid Solar.* [Interview]. 2013.

[17] National Renewable Energy Laboratory, "PV Watts: Changing System Parameters," [Online]. Available: http://rredc.nrel.gov/solar/calculators/PVWATTS/version1/change.html#derate. [Accessed 2013].

[18] D. R. Myers, "Solar radiation modeling and measurements for renewable energy applications: data and model quality," *Elsevier Energy*, no. 30, pp. 1517-1531, 2005.

[19] T. Mosher, "Economic Valuation of Energy Storage Coupled with Photovoltaics: Current Technologies and Future Projections," Massachusetts Institute of Technology, 2010.

[20] I. Hadjipaschalis, A. Poullikkas and V. Efthimiou, "Overview of current and future energy storage technologies for electric power applicaitons," *Elsevier,* 2009.

[21] UL, "Safety Issues for Lithium-Ion Batteries," 2012.

[22] D. K. Nichols and S. Echroad, "Utility-Scale Application of Sodium Sulfur Battery".

[23] R. A. Muller, Energy for Future Presidents, New York, NY: W. W. Norton & Company, Inc., 2012.

[24] D. Enos and J. Wood, "Carbon-Enhanced Lead-Acid Batteries," U.S. Department of Energy, Sandia National Laboratories, 2012.

[25] Advanced Lead-Acid Battery Consortium, "Achievements," 2011. [Online]. Available: http://www.alabc.org/achievements. [Accessed 2013].

[26] T. Crompton, Battery Reference Book, Second Edition, Butterworth-Heinemann Ltd., 1995.

[27] P. de Boer and J. Raadshelders, "Flow batteries," Leonardo Energy, 2007.

[28] L. Joerissen, J. Garche, C. Fabjan and G. Tomazic, "Possible use of vanadium redox-flow batteries for energy storage in small grids and stand-alone photovoltaic systems," *Elsevier Journal of Power Sources,* no. 127, pp. 98-104, 2004.

[29] C. Blanc and A. Rufer, "Understanding the Vanadium Redox Flow Batteries," in *Paths to Sustainable Energy* , InTech, 2010.

[30] T. Nguyen and R. F. Savinell, "Flow batteries," The Electrochemical Society, 2010.

[31] Ameren Missouri, "Taum Sauk Plant," [Online]. Available: http://www.ameren.com/sites/aue/Media/Pages/TaumSaukInformation.aspx. [Accessed 2013].

[32] T. Lipman, "An Overview of Hydrogen Production and Storage Systems with Renewable Hydrogen Case Studies," Clean Energy States Alliance, Montpelier, VT, 2011.

[33] H. Bindner, T. Cronin, P. Lundasager, J. F. Manwell, U. Abdulwahid and I. Baring-Gould, "Lifetime Modelling of Lead Acid Batteries," Riso National Laboratory, Roskilde, Denmark, 2005.

[34] D. C. Jordan and S. R. Kurtz, "Photovoltaic Degradation--An Analytical Review," National Renewable Energy Laboratory, Golden, CO, 2012.

[35] Ameren Missouri, *Typical Missouri Home,* Ameren Missouri, 2011.

[36] Battery University, "Basics About Discharging," 2013. [Online]. Available: http://batteryuniversity.com/learn/article/discharge_methods. [Accessed 2013].

[37] H. Yang, L. Lu and W. Zhou, "A novel optimization sizing model for hybrid solar-wind power generation system," *Elsevier,* 2006.

[38] S. Schoenung, "Energy Storage Systems Cost Update," Sandia National Laboratories, Albuquerque, NM, 2011.

[39] K. Chatzivasileiadi, "Electrical energy storage technologies and the built environment," International Renewable Energy Storage Conference.

[40] K. Bradbury, "Energy Storage Technology Review," 2010.

[41] J. Eyer, "Benefits from Flywheel Enegy Storage for Area Regulation in California--Demonstration Results," Sandia National Laboratories, Albuquerque, NM, 2009.

[42] Bureau of Labor Statistics, "Consumer Price Index," U.S. Department of Labor, 2013. [Online]. Available: http://www.bls.gov/cpi/. [Accessed 2013].

[43] J. M. Eyer, J. J. Iannucci and G. P. Corey, "Energy Storage Benefits and Market Analysis Handbook," Sandia National Laboratories, Albuquerque, NM, 2004.

[44] U.S. Census Bureau, "Median and Average Square Feet of Floor Area in New Single-Family Houses Completed by Location".

[45] U.S. Census Bureau, "Lot Size of New Single-Family Houses Sold".

[46] V. M. Fthenakis, H. C. Kim and E. Alsema, "Emissions from Photovoltaic Life Cycles," *Environmental Science Technology*, no. 42, pp. 2168-2174, 2008.

[47] J. L. Sullivan and L. Gaines, "A Review of Battery Life-Cycle Analysis: State of Knowledge and Critical Needs," Argonne National Laboratory, Oak Ridge, TN, 2010.

[48] National Renewable Energy Laboratory, "Life Cycle Greenhouse Gas Emissions," National Renewable Energy Laboratory, Golden, CO, 2012.

[49] D. Hsu, P. O'Donoughue, V. Fthenakis, G. Heath, H. Kim, P. Sawyer, J. Choi and D. Turney, "Life Cycle Greenhouse Ga Emissions of Crystalline Silicon Photovoltaic Electricity Generation: Systematic Review and Harmonization," *Journal of Industrial Ecology*, pp. S122-S135, 2012.

[50] M. Whitaker, G. Heath, P. O'Donoughue and M. Vorum, "Life Cycle Greenhouse Gas Emissions of Coal-Fired Electricity Generation: Systematic Review and Harmonization," *Journal of Industrial Ecology*, pp. S53-S72, 2012.

[51] Oxford Dictionaries, Oxford University Press., 2013.

VITA

I am Brian Peterson. I completed my B.S. degree in Chemical Engineering with a minor in Mathematics at Missouri University of Science and Technology in December 2011. After participating the National Science Foundation's Research Experience for Undergraduates (REU) program at the Center for Sustainable Energy at Kansas State University under the direction of Dr. Peter Pfromm and Dr. Ronald Michalsky in Summer 2011, I decided to pursue an advanced degree.

I approached Dr. Joseph D. Smith, director of Missouri S&T's ERDC, expressing interest in researching alternative energy sources. I became one of Dr. Smith's graduate research assistants as part of completion of my M.S. in Chemical Engineering (December 2013). I also was a graduate teaching assistant and a course instructor for the Chemical Engineering Department.